

**UNIVERSITÀ DEGLI STUDI DI NAPOLI FEDERICO II**



**DOTTORATO DI RICERCA IN**

**MEDICINA CLINICA E SPERIMENTALE**

*CURRICULUM IN SCIENZE IMMUNOLOGICHE E DERMATOLOGICHE*

**XXIX Ciclo**

**Coordinatore: Prof. Gianni Marone**

**TESI DI DOTTORATO**

**TITOLO**

**N-FORMYL PEPTIDE RECEPTORS AND uPAR FOSTER  
THE OXIDATIVE STRESS IN SYSTEMIC SCLEROSIS**

TUTOR/RELATORE

**Chiar.ma Prof.ssa Nunzia Montuori**

CANDIDATA

**Dott.ssa Filomena Napolitano**

## INDICE

<b>1. Abstract</b>	4
<b>2. Introduction</b>	5
2.1 Systemic Sclerosis: general aspects	5
2.2 Pathogenesis of Systemic Sclerosis	5
2.3 Oxidative stress in Systemic Sclerosis	7
2.4 The <i>N</i> -formyl peptide receptors (FPRs)	9
2.5 FPRs signal transduction pathways	10
2.6 FPRs role in human diseases	12
2.7 The urokinase-type plasminogen activator receptor (uPAR): a versatile signaling orchestrator	13
2.8 uPAR functions	14
2.9 uPAR forms	15
2.10 uPAR molecular interactions and signaling	16
2.11 Aim of study	18
<b>3. Materials and Methods</b>	19
3.1 Peptides and chemicals	19
3.2 Tissues and patients samples	20
3.3 Cell cultures	21
3.4 RNA purification and analysis	22
3.5 Western blot analysis	22
3.6 Co-immunoprecipitation	23
3.7 Determination of ROS	23
3.8 Flow cytometric analysis of surface molecules	24
3.9 Determination of Rac1 activity and association with p67 <sup>phox</sup>	25
3.10 Histology and immunohistochemistry	25
3.11 Statistical analysis	26
<b>4. Results</b>	27
4.1 <i>In vivo</i> expression of FPR1, FPR2, and FPR3 in human normal and SSc skin fibroblasts	27
4.2 <i>In vitro</i> expression of FPR1, FPR2, and FPR3 in human normal and SSc skin fibroblasts	27
4.3 <i>In vivo</i> and <i>in vitro</i> expression of uPAR forms in human skin fibroblasts	28
4.4 Expression of FPRs in human normal fibroblasts; uPAR expression and direct interaction with FPR1 in human normal foreskin fibroblasts	30
4.5 Effects of fMLF, WKYMVm peptide, and uPAR <sub>84-95</sub> on ROS production in	

human normal foreskin fibroblasts_____	31
4.6 FPRs-uPAR-Integrin crosstalk as a potential player in ROS generation by human normal foreskin fibroblasts_____	32
4.7 Rac1 and ERK1/2 pathways are involved in ROS production after FPRs stimulation in human normal foreskin fibroblasts_____	33
4.8 FPRs induce ROS production through the upregulation and activation of NADPH oxidase-2 in human normal foreskin fibroblasts_____	34
4.9 FPRs mediated ROS production in human normal and SSc Skin fibroblasts____	35
4.10 Therapeutic strategies to modulate FPRs/uPAR-mediated generation of oxidative stress by fibroblast cells_____	36
<b>5. Conclusions_____</b>	<b>38</b>
<b>6. Figures_____</b>	<b>42</b>
<b>7. References_____</b>	<b>57</b>

## 1. ABSTRACT

Systemic sclerosis (SSc) is characterized by chronic inflammation and fibrosis. *N*-Formyl peptide receptors (FPRs) are chemotactic receptors involved in inflammation. Three FPRs have been identified: FPR1, FPR2, and FPR3.

We have examined, by RT-PCR, Western blot and immunohistochemistry, FPRs expression in skin fibroblasts from normal subjects and SSc patients, showing an increased expression in SSc fibroblasts.

Several functions of FPRs occur through the interaction with the chemotactic domain (residues <sup>88</sup>SRSRY<sup>92</sup>) of the urokinase-type plasminogen activator receptor (uPAR). Western blot and immunohistochemistry analysis also showed an increased expression in SSc fibroblasts of a cleaved uPAR form exposing the SRSRY sequence at its N-terminus (DIIDIII-uPAR<sub>88-92</sub>).

We demonstrated that FPRs stimulation promoted radical oxygen species (ROS) generation in normal and SSc fibroblasts. Upon stimulation, ROS production was due to FPRs interaction with uPAR and to  $\beta_1$  integrin engagement. FPRs cross-talk with uPAR and integrins led to Rac1 and ERKs activation. Rac1 is a cytosolic component of the NADPH oxidase system. Active GTP-Rac1 binds to p67<sup>phox</sup> that translocates to the membrane and associates with the catalytic gp91<sup>phox</sup>. FPRs stimulation promoted gp91<sup>phox</sup> and p67<sup>phox</sup> expression as well the direct interaction between GTP-Rac1 and p67<sup>phox</sup> in fibroblast cells.

Finally, we were able to show that C37, a new small molecule inhibiting the structural and functional interaction between FPRs and uPAR, and Selumetinib, a clinically approved MAPKK/ERK inhibitor, blocked FPRs-mediated ROS production in fibroblasts, thus suggesting new therapeutic strategies for the treatment of fibrosis in SSc.

## **2. INTRODUCTION**

### **2.1 Systemic Sclerosis: general aspects**

Systemic Sclerosis (SSc), also known as Scleroderma, is a chronic multisystem autoimmune disease characterized by excessive deposition of collagen and other connective tissue macromolecules in the skin and in multiple internal organs, severe alteration in the microvasculature and immunologic abnormalities. It is a rare but severe disorder characterized by clinical heterogeneity, an unpredictable course, high mortality and resistance to therapy (1, 2). Clinical forms range from limited skin involvement with minimal systemic alterations (lcSSc) to forms with diffuse skin sclerosis and severe internal organ disease (dcSSc) (3).

The studies of the prevalence and incidence of SSc indicate a prevalence ranging from 50 to 300 cases per 1 million persons and an incidence ranging from 2.3 to 22.8 cases per 1 million persons per year. Woman (age range between 30 and 50 years) are at much higher risk for scleroderma than men, with a ratio ranging from 3:1 to 14:1. The survival rate is between 34 and 76% and is strictly related to the level of internal organs involvement (4).

### **2.2 Pathogenesis of Systemic Sclerosis**

The pathogenesis of SSc is extremely complex and remains not fully understood. At present, no single unifying hypothesis explains all aspects of its pathogenesis. However, fundamental abnormalities in at least 3 types of cells are involved in the development of the clinical and pathologic manifestations of the disease: 1) fibroblasts; 2) endothelial cells; 3) innate immune cells, particularly T and B lymphocytes (Fig. 1).

The functional alterations in these cells determine progressive cutaneous and visceral fibrosis, vascular lumen obliteration, immunologic dysregulation, which include the production of numerous autoantibodies, the chronic mononuclear-cell infiltration of affected tissues, the dysregulation of lymphokine and growth factor production (2).

At present, it is not yet clear which alteration is of primary importance in SSc and despite a number of studies that examined several aspects of its intricate picture, the mechanisms involved are still largely unknown. During the past decade, considerable attention has been paid to the origin of myofibroblast, the mesenchymal cell type most responsible for the excessive matrix production and deposition in tissue and vessel wall, found in fibrotic disorders and fibroproliferative vasculopathies (5). However, in SSc, the origin of myofibroblasts has not been completely elucidated. In fibrotic diseases, myofibroblasts may derive from at least three sources: 1) expansion and activation of resident tissue fibroblasts; 2) transition of epithelial cells into mesenchymal cells, a process known as epithelial–mesenchymal transition (EMT); and 3) tissue migration of bone marrow–derived circulating fibrocytes (6).

Under normal circumstances, the fibroblast repair program is self limited, but pathological fibrotic responses are characterized by sustained and amplified fibroblast activation (5) (Fig. 2). In SSc, uncontrolled fibroblasts activation, accumulation of myofibroblasts in affected tissues and their biosynthetic functions are crucial determinants of the extent and rate of fibrosis and influence significantly the clinical course of the disease as well as the response to therapy, thus dictating the prognosis and the overall mortality (5).

Fibroblasts acquiring a myofibroblast phenotype express typical mesenchymal markers, such as  $\alpha$ -smooth muscle actin ( $\alpha$ -SMA), vimentin, and type I collagen. Besides the acquisition of an activated profibrogenic phenotype, these cells also become motile and capable of migrating into surrounding tissues (5, 6).

Recently, endothelial mesenchymal transition (EndoMT), a newly recognized type of cellular trans-differentiation, has emerged as another possible source of tissue myofibroblasts, deeply involved in the pathogenesis of fibrotic disease (7).

### **2.3 Oxidative stress in Systemic Sclerosis**

Several years ago, the pathogenesis of SSc was linked to the presence of a large excess of reactive oxygen species (ROS). This hypothesis, over the years, has been supported by numerous reports which documented the presence of an abnormal redox state in SSc patients and several other fibrotic disorders (8, 9).

Although the role of ROS-induced oxidative stress in the pathogenesis of SSc has not been studied as extensively, it has been shown that ROS contribute to the persistent fibrotic phenotype of SSc fibroblasts (10) and that antioxidants, such as epigallocatechin-3gallate, can reduce extracellular component matrix (ECM) production, function, and activity of dermal fibroblasts from SSc patients (11).

Among the major source of ROS, nicotinamide adenine dinucleotide phosphate (NADPH) oxidases have been demonstrated to play a fundamental role in ROS production and in the redox signaling (12). The NADPH oxidase (also called Nox) complex was originally identified in phagocytic leukocytes as an enzymatic defense system against infections required for the oxidative burst-dependent microbial killing. It is composed of membrane-associated and cytosolic components, which assembly to form the active Nox enzymatic complex in

response to appropriate stimuli. Specifically, this complex consists of membrane-associated cytochrome b558, comprising the catalytic gp91<sup>phox</sup> (also known as Nox2) and regulatory p22<sup>phox</sup> subunits, and four cytosolic regulatory components, including p40<sup>phox</sup>, p47<sup>phox</sup>, p67<sup>phox</sup> and the small GTPase Rac1. Upon stimulation, p47<sup>phox</sup> is phosphorylated and forms a complex with the other cytosolic subunits. This complex migrates to the cell membrane where it combines with cytochrome b558 to constitute the active enzyme which transfers electrons from a substrate to O<sub>2</sub>, generating O<sub>2</sub><sup>-</sup> (13).

Subsequently, NADPH oxidase complexes were also found in nonphagocytic cells, where several isoforms of the catalytic Nox2 protein were identified, including Nox1, Nox3, Nox4, Nox5, Duox1 and Duox2. The expression of the catalytic subunits varies among different cell types, and it has become clear that generated ROS modulate a variety of cellular functions, including proliferation, migration, cell contraction, growth, apoptosis, and senescence (14).

It is known that processes such as inflammation, ischemia or hypoxia are characterized by a significant increase in ROS production through the activation of NADPH oxidase. In fact, molecules such as VEGF, PDGF, TGF-β, angiotensin II and thrombin, all significantly higher in SSc patients than in controls, are able to stimulate the various subclasses of Nox family present in vascular smooth muscle cells and fibroblasts (15). In these cells, the redox state may play a significant role in the progression of fibrosis through an auto-amplification circuit linking ROS, Ras and ERK 1/2 which in turn amplifies and maintains the autocrine loop made up by cytokines, growth factors and their cognate receptors. For this reason, inappropriate NADPH oxidase activation seem to play a

fundamental role in determining events such as pulmonary hypertension, renal crisis and skin fibrosis (12).

The evidence of platelet derived growth factor receptor (PDGFR) agonistic autoantibodies in the sera of SSc patients and the finding of their ability in inducing ROS from monocytes and fibroblasts has provided a novel clue to the pathogenesis of the disease (16).

Thus, the study of the molecular mechanisms of ROS generation and involvement in the pathogenesis of SSc may lead to the development of novel treatments potentially transferable to the therapy of scleroderma patients.

#### **2.4 The N-formyl peptide receptors (FPRs)**

Leukocytes infiltration at sites of inflammation and infection is dependent on the presence of a gradient of chemotactic factors or chemoattractants. Synthetic *N*-formyl-methionyl-leucyl-phenylalanine (fMLF) was one of the first identified highly potent chemoattractants for leukocytes. In 1976, a high-affinity binding site was found on the cell surface of neutrophils for the prototypic fMLF, and was biochemically defined formyl peptide receptor (FPR) (17). Subsequently, using a FPR cDNA probe, two other human genes were isolated by hybridization and called FPRL1 (formyl peptide receptor like 1) and FPRL2 (formyl peptide receptor like 2), which were shown to cluster with FPR on human chromosome 19q13.3–19q13.4. FPRL1, also termed lipoxin A4 (LXA4) receptor ALX, is a low-affinity receptor for fMLF, based on its *in vitro* activation by high concentrations ( $\mu\text{M}$ ) of fMLF. FPRL2 does not bind or respond to *N*-formyl peptides, but instead shares some non-formylated chemotactic peptide ligands with FPRL1 (18).

In 2009, the International Union of Basic and Clinical Pharmacology named the formyl peptide receptor subtypes FPR, FPRL1, and FPRL2 to FPR1, FPR2/ALX, and FPR3, respectively (19).

FPRs belong to a class of G-protein-coupled receptors (GPCRs) involved in host defense against pathogens in the innate immune system. FPRs function is best known in phagocytic leukocytes (*e.g.* neutrophils and monocytes) that, in response to microbial chemoattractants, migrate and accumulate at sites of infection, where they release ROS and other factors to combat invading microorganisms (18).

FPR1, namely the high affinity receptor, is activated by nanomolar concentrations of fMLF. FPR2 is a promiscuous receptor activated in response to high concentration of fMLF, viral peptides (gp41 envelope protein of the HIV-1 virus), bacterial peptides (Hp<sub>2-20</sub>, a non-formyl peptide derived from *Helicobacter pylori*), endogenous peptides [Amyloid beta (1–42) fragment, prion protein fragment PrP(106–126), cleaved soluble fragments of Urokinase-type plasminogen activator receptor (uPAR)], and synthetic peptides. Hp<sub>2-20</sub> (20), and F2L (21) are natural ligands for FPR3. The synthetic peptide WKYMVm is mainly a FPR2 and FPR3 agonist (20) (Fig. 3).

Although FPRs expression has been initially described in immune cells, it is becoming increasingly clear that FPRs are also expressed in other cell types and tissues (22).

### **2.5 FPRs signal transduction pathways**

FPRs are G protein-coupled receptors (GPCRs) that can be inhibited by pertussis toxin indicating that the G proteins associated with these receptors belong to the G<sub>i</sub> family (18).

It has been well established that GPCRs are subjected to desensitization. ‘Homologous desensitization’ is rapidly induced by binding of cognate agonists in association with receptor phosphorylation and internalization (19). These receptors may also be ‘heterologously’ desensitized by agonists that activate other unrelated receptors; receptor desensitization relies mainly on G protein-coupled receptor kinases (GRKs) family-mediated receptor phosphorylation (18).

However, receptor phosphorylation alone is not enough to prevent G protein binding and activation. For homologous desensitization, the binding of arrestins with phosphorylated receptor prevents G protein binding, leading to receptor inactivation (23).

FPRs activate distinct patterns of intracellular signaling indicating that selective activation of intracellular signaling cascades may underlie different functional responses (24). After binding of its agonists, FPRs activate the heterotrimeric G protein, which dissociates into  $\alpha$  and  $\beta\gamma$  subunits, activating the phospholipase C (PLC) and the phosphatidylinositol 3-kinase (PI3K) (25). Hydrolysis of phosphatidylinositol 4, 5-bisphosphate (PIP<sub>2</sub>) by PLC generates IP<sub>3</sub>, which releases calcium from endoplasmic reticulum stores. The release of calcium is a necessary condition for the chemotaxis of neutrophils (26). Hydrolysis of phosphatidylinositol 4, 5-bisphosphate (PIP<sub>2</sub>) by PLC also generates diacylglycerol (DAG), which activates various isoforms of protein kinase C (PKC).

The phosphatidylinositol 3-kinase (PI3K) - Akt / PKB pathway is also activated, in particular the PI3K $\gamma$ , which is the isoform more associated with chemoattractant receptors. Other intracellular events include: the activation of CD38, a surface glycoprotein which, acting on NAD<sup>+</sup>, activates a cascade of

events that lead to increased concentrations of cyclic AMP (cAMP) and the release of  $\text{Ca}^{2+}$  at the extracellular level, phospholipase A2 and D, RAS-dependent activation of the mitogen-activated protein kinases (MAPK) ERK1/ERK2, JNK and p38MAPK cascade and also some other protein tyrosine kinases. In particular, the MAPK cascade is involved in several physiological processes including growth, differentiation and cell migration, apoptosis and immune responses (27).

One of the most important biochemical responses triggered by FPRs stimulation is the activation of the multimeric complex of the NADPH oxidase. ERKs are involved in the phosphorylation of  $\text{p47}^{\text{phox}}$  and represent one target of PKC in the signal transduction pathway activated by FPRs.  $\text{p47}^{\text{phox}}$  cytosolic subunit can be considered a regulatory subunit of the enzyme complex, because its phosphorylation allows the translocation of cytosolic components of the NADPH oxidase complex (28).

An additional control of NADPH oxidase activation is determined by the GTPase Rac1/2, which, directly interacts with the N-terminal tetratricopeptide repeat (TPR) domain of  $\text{p67}^{\text{phox}}$  (29, 30) and serves as an “adaptor” by providing a stable platform for the interaction with the catalytic component  $\text{gp91}^{\text{phox}}$ .

## **2.6 FPRs role in human diseases**

Accumulating evidences show that FPRs possess important regulatory effects in multiple diseases including inflammation, amyloidosis, Alzheimer’s disease, prion disease, acquired immunodeficiency syndrome, obesity, diabetes and cancer (27). FPRs are expressed in abundance on cells of the host defence system; however, they may have distinctly different functions beyond simple pathogen recognition.

The ability of FPRs to recognize endogenous ligands appears to be essential for the regulation of non-infectious inflammation, wound healing and tissue regeneration. Recently, FPRs involvement was described in the repair of intestinal, gastric and nasal epithelial cells after inflammatory processes (27).

FPRs seem to exert homeostatic functions in epithelia. Alterations in the colonic film mucin layer, increased epithelial permeability and defective mucosal wound healing have been observed in FPR1<sup>-/-</sup> mice during chronic dextran sodium sulphate (DSS)-induced colitis. Furthermore, knockout of FPR2 in mouse colon epithelial cells impaired mucosal recovery after damage (27).

Moreover, FPRs activation promotes angiogenesis in various inflammatory settings in response to both exogenous and endogenous ligands. FPRs also exert a complex role in cancer. They inhibit tumor growth and/or the angiogenic response in both the stomach and colon; by contrast, in glioblastoma models, FPR1 is needed to stimulate angiogenesis and tumor growth (31).

Both in inflammatory and epithelial cells, FPRs exert their action through a structural and functional interaction with the urokinase-type plasminogen activator (uPA) receptor (uPAR). How these receptors interact to recognize their ligands, transduce their signals and contribute to disease pathogenesis are basic questions currently under investigation that would open up new avenues for the future management of inflammation-related diseases.

## **2.7 The urokinase receptor: a versatile signaling orchestrator**

The urokinase-type plasminogen activator receptor (uPAR) is a glycosyl-phosphatidyl-inositol (GPI)-anchored cell-surface receptor involved in many physiological and pathological events which require remodeling of the

extracellular matrix, such as embryogenesis, inflammation, tumor invasion and metastasis (32). uPAR traditional role was considered the focusing of the urokinase (uPA) proteolytic activity on the cell surface; however, different uPAR activities have been demonstrated in the last years. Indeed, despite the lack of a transmembrane domain, uPAR can activate intracellular signaling through lateral interactions with other cell surface receptors, such as integrins, receptor tyrosine kinases, and G-protein-coupled chemotaxis receptors (33).

uPAR itself is an adhesion receptor; it binds directly vitronectin (VN), a protein of the provisional ECM (34).

## **2.8 uPAR functions**

uPAR is a single chain glycoprotein which binds uPA with high affinity ( $K_d = 10^{-10}$  M) and concentrates the activity of the enzyme to the cell surface. The receptor also binds, with the same affinity, the inactive form of urokinase (pro-uPA), facilitating its activation (35).

uPAR is synthesized as a single polypeptide chain of 313 amino acids and undergoes a post-translational maturation process during which, at the C-terminal, a peptide of 30 amino acids is removed and a GPI tail is added. This tail is essential for anchoring of receptor to the plasma membrane and allows uPAR association with the plasma membrane rich in cholesterol microdomains, also called "lipid rafts", involved in signal transduction.

uPAR molecular weight is between 50 and 60 kDa; the heterogeneity depends on the presence of 5 potential sites of *N*-glycosylation that modulate the affinity of the receptor for their ligands (35).

The mature receptor is formed by three homologous domains (DI, DII, and DIII, numbered from the N-terminus). DIII domain anchors the receptor to the membrane through the GPI tail, DII domain connects DIII to the N-terminal DI, which interacts with the amino-terminal fragment (ATF) of uPA.

uPA is a serine protease which cleaves plasminogen, generating the active protease plasmin. Plasmin cleaves and activates matrix metalloproteases (MMPs). Both plasmin and MMPs degrade many ECM components and activate growth factors or liberate them from ECM sequestration.

uPA can also induce a cascade of intracellular signaling independent of its catalytic activity. These effects are mediated by uPA binding, in active or inactive form (pro-uPA), to uPAR, through which, uPA can stimulate cell growth, motility, adhesion, and transcription of specific genes (35).

uPAR also binds the somatomedin B domain of VN through a specific binding domain exposed on the DI/DII interface of the receptor (34). uPAR promotes metastasis of human malignancies by engaging VN through the activation of a cell signaling to Rac-1 and induces phenotypic changes consistent with hypoxia-induced EMT (34, 36) (Fig. 4A).

## **2.9 uPAR forms**

uPAR can be cleaved between domains DI and DII, thus generating a soluble DI fragment and membrane anchored DIIDIII-uPAR forms.

The release of domain DI occurs following a proteolytic cleavage by several proteases including trypsin, chymotrypsin, elastase, cathepsin G, plasmin and uPA itself. uPA can cut uPAR in two sites: Arg<sup>83</sup>-Ala<sup>84</sup> and Arg<sup>89</sup>-Ser<sup>90</sup>. A cut in the Arg<sup>83</sup>-Ala<sup>84</sup> site leads to the N-terminal exposure of an epitope corresponding to

amino acids 88-92 (SRSRY), thus generating the DIIDIII-uPAR<sub>88-92</sub>, able to interact with FPRs and involved in cell migration (Fig. 4A). A cut in the second site destroys the SRSRY region and generates DIIDIII-uPAR, unable to interact with FPRs.

In addition to the membrane-anchored uPAR, soluble receptor forms (suPAR, DIIDIII-suPAR<sub>88-92</sub>, DIIDIII-suPAR) are released after cleavage of the GPI anchor by phospholipase C or D (37) (Fig. 4B).

### **2.10 uPAR molecular interactions and signaling**

The identification of transmembrane receptors that cooperate with uPAR has contributed to elucidate the uPAR-dependent cell signaling mechanisms. In fact, the stimulation of uPAR regulates adhesion, migration and cell proliferation, protects against apoptosis and anoikys, and induces EMT, independently from uPA enzymatic activity (38).

uPAR can activate intracellular signaling through lateral interactions with other cell surface receptors, such as integrins, receptor tyrosine kinases, and FPRs. uPAR ability to regulate integrin activity plays a key role in cell adhesion, migration, proliferation, and survival. Integrin-binding sites have been identified in uPAR domain DII (peptide D2A, residues 130–142) and in uPAR domain DIII (residues 240–248). Soluble D2A abolishes uPAR- $\alpha$ v $\beta$ 3 and uPAR- $\alpha$ 5 $\beta$ 1 co-immunoprecipitation, indicating that it can bind both of these integrins; in addition, D2A has chemotactic activity that requires  $\alpha$ v $\beta$ 3 and activates  $\alpha$ v $\beta$ 3 signaling pathways (39). The specific sequence identified in the uPAR domain DIII binds the  $\alpha$ 5 $\beta$ 1 integrin; substituting a single amino acid in that region (S245A) impairs uPAR binding to the purified integrin (40).

As for VN and uPA binding, the uPAR/integrin association requires the intact 3-domain structure of uPAR (41).

uPAR-integrin interactions activates the MAPK cascade, in particular ERK 1/2, with the involvement of non-receptor tyrosine kinase src, tyrosine-kinase family src (Hck, Fgr, Fyn) and focal adhesion-associated protein kinase (FAK). Activation of these intracellular mediators then lead to different results depending on the cell type (38).

uPAR interaction with FPRs occurs at the cell surface and is required for both uPA- and fMLF-dependent cell migration. Cross-talk between uPAR and FPRs occurs through a chemotactic domain located in the DI–DII linker region of uPAR, the SRSRY sequence (amino acids 88–92) exposed upon proteolytic cleavage of the receptor (42).

It has been proposed that the SRSRY sequence is masked in cell-surface uPAR and that uPA binding to uPAR determines a conformational modification of the receptor with the exposure of the chemotactic SRSRY domain that, in turn, binds and activates FPRs, thus inducing chemotaxis (43).

A soluble cleaved form of uPAR, lacking the DI domain and exposing at the N-terminus the SRSRY sequence, was also identified as a ligand for FPRs in human plasma and urine (44).

uPAR interacts with several other molecules such as growth-factor receptors as the receptors for the epidermal growth factor (EGFR) and for the PDGFR-beta, which appear to mediate uPAR-associated proliferative signal (38).

### **2.11 Aim of study**

SSc is characterized by severe and often progressive fibrosis of the skin and multiple internal organs. The mechanisms responsible for these alterations remain obscure, although excessive ROS-mediated oxidative stress has been implicated.

This research project, starting from recent experimental evidences demonstrating the involvement of the innate immunity receptors in the pathogenesis of chronic inflammatory diseases, has the aim to clarify a possible role of FPRs and their cross-talk with uPAR in ROS production in normal and SSc skin fibroblasts.

Furthermore, this study was also undertaken to elucidate the intracellular signaling pathways involved in ROS generation and to analyze the effects of the cross-talk between FPRs/uPAR/ $\beta$ 1 integrin on FPRs-mediated ROS production in fibroblast cells.

The identification of specific factors or pathways involved in the deregulation of the fibrotic process offers the potential for the development of therapeutic strategies for fibrotic diseases, which are still characterized by high morbidity and mortality.

## 3 MATERIALS AND METHODS

### 3.1 Peptides and chemicals

The hexapeptide Trp-Lys-Tyr-Met-Val-D-Met-NH<sub>2</sub> (WKYMVm) was synthesized and HPLC purified (95%) by Innovagen (Lund, Sweden), the peptide uPAR<sub>84-95</sub> was synthesized by PRIMM (Milan, Italy), uPA N-terminal fragment (ATF-uPA) was from American Diagnostica (Greenwich, CT) and *N*-Formyl-L-methionyl-L-leucyl-L-phenylalanine (fMLF) was from Calbiochem (La Jolla, CA). TRIzol solution was from Invitrogen FischerScientific (Illkirch, France), and DNA ladder and Moloney leukemia virus reverse transcriptase were from Promega (Madison, WI). Protein concentration was estimated with a modified Bradford assay (Bio-Rad Laboratories). ECL Plus was from GE Healthcare (Buckinghamshire, UK), and 29,79-dichlorodihydrofluorescein diacetate (DCHF-DA) was from Molecular Probes (Invitrogen, Paisley, UK). The mixture of protease and phosphatase inhibitors was from Calbiochem. Mouse anti-FPR1, rabbit anti-FPR2, mouse anti-FPR3, mouse anti-gp91<sup>phox</sup>, rabbit anti-p67<sup>phox</sup>, mouse anti phospho-ERK and rabbit anti ERK 2 were from Santa Cruz Biotechnology (Santa Cruz, CA); mouse anti-tubulin and rabbit anti-actin were from Sigma-Aldrich (St. Louis, MO); rabbit anti-uPAR<sub>84-95</sub> (also called IB in the text) was from PRIMM; mouse anti-Rac1 was from Upstate Biotechnology (Lake Placid, NY); mouse monoclonal anti-uPAR ADG3937 was from American Diagnostica; mouse monoclonal R3 and mouse monoclonal R4 were kindly provided by Gunilla Høyer-Hansen (Finsen Laboratory, Copenhagen, Denmark). Secondary anti-mouse and anti-rabbit Abs coupled to HRP were from Bio-Rad (Munich, Germany). PD98059 and NSC23766 were from Calbiochem, P25 from PRIMM, Selumetinib (AZD6244) from AstraZeneca and C37 from the NCI/DTP Open Chemical Repository (Available from: <http://dtp.cancer.gov>);

they were dissolved in dimethyl sulfoxide (DMSO), stored at  $-20^{\circ}\text{C}$ , and added to the culture at final concentrations indicated in the text.

### **3.2 Tissues and patients samples**

Eight females and two males affected by SSc, observed from January 2011 to December 2013 in the Day Hospital of the Department of Translational Medical Sciences of the University of Naples Federico II, were classified according to the American College of Rheumatology criteria (45) as having limited cutaneous SSc (lcSSc;  $n = 6$ ) or diffuse cutaneous (dcSSc;  $n = 4$ ) (3) and included in the study. All patients signed a written informed consent according to the guidelines of the institutional review board for the use of humans in research. The mean age of patients was 54 y (range, 31–70 y). Disease duration was calculated from the time of onset of the first clinical event (other than Raynaud's phenomenon) that was a clear manifestation of SSc. Patients were classified as having an early-stage ( $n = 4$ ) or late stage ( $n = 6$ ) SSc, according to disease duration ( $<5$  y for early-stage limited cutaneous SSc and  $<3$  y for early-stage diffuse cutaneous SSc) and skin histopathology (46). We considered clinically involved skin for values of skin thickness  $\geq 2$ , according to the modified Rodnan skin thickness score. All patients with the diffuse form had involvement of dorsal arm and/or thorax. To reduce variability among the patients, we admitted for study only SSc patients positive for antinuclear Abs, showing a speckled pattern as evaluated by indirect immunofluorescence and ELISA. Because antinuclear Ab positivity may be considered not sufficient for subtype characterization, other clinical measures were investigated; in particular, all patients with diffuse cutaneous SSc presented anti-SCL-70 topoisomerase I positivity, and patients with limited cutaneous SSc showed serum anticentromere (CENP-B) positivity. All patients were washed out from steroid treatment 30 d before

the biopsy was taken. Other treatments were allowed (proton pump inhibitors, vasodilators, and so on). Patients who could not undergo washout because of the severe organ complications were not evaluated. Patients with symptoms overlapping with those of other autoimmune, rheumatic, and/or connective tissue diseases were excluded from the study. Control donors were matched with each scleroderma patient for age, sex, and biopsy site, and control samples were processed in parallel control (eight females and two males; mean  $\pm$  SD age,  $43 \pm 15$  y).

### **3.3 Cell cultures**

Surgical fragments were mechanically dissociated under a light microscope and subjected to trypsinization for 30 min at 37°C, as described previously (47). After two PBS washings, cells were plated and cultured in monolayer in DMEM (Life Technologies Carlsbad, CA) supplemented with 10% heat inactivated FBS (Life Technologies), 100 U/ml penicillin G sodium, and 100 mg/ml streptomycin sulfate, at 37°C, in a humidified atmosphere of 5% CO<sub>2</sub>. Fibroblasts from normal subjects and from patients with SSc were used between the 3rd and 10th passage in culture.

The BJ (human foreskin fibroblasts), the HGF-1 (human gingival fibroblasts) and the MRC-5 (human lung fibroblasts) were from ATCC (LGC Standards, Milan, Italy) and were grown in DMEM (Life Technologies) supplemented with 10% FBS.

BJ cells, on which we have focused our studies, were obtained from ATCC at the 6<sup>th</sup> passage, subcultured and frozen in stock vials; they were used between the 1<sup>st</sup> and 10<sup>th</sup> passage in culture.

The H460 (cell lung cancer) were obtained from ATCC and grown in RPMI 1640 medium (Life Technologies) supplemented with 10% FBS.

### **3.4 RNA purification and analysis**

Total cellular RNA was isolated by lysing cells in TRIzol solution, according to the supplier's protocol (43). RNA was precipitated and quantitated by spectroscopy. Five micrograms of total RNA was reversely transcribed with random hexamer primers and 200 U murine Moloney leukemia virus reverse transcriptase. One microliter of reverse-transcribed DNA was then amplified for FPR1, FPR2, FPR3, and GAPDH using specific primers. The primers for FPR1 were 5'-ATGGAGACAAATTCCTCTCTC (sense) and 3'-CACCTCTGCAGAAGGTAAAGT (antisense); for FPR2 were 5'-CTTGTGATCTGGGTGGCTGGA (sense) and 3'-CATTGCCTGTAACTCAGTCTC (antisense) (43); and for FPR3 were 5'-AGTTGCTCCACAGGAATCCA (sense) and 3'-GCCAATATTGAAGTGGAGGATCAGA (antisense) (48). The primers for GAPDH were 5'-GCCAAAGGGTCATCATCTC (sense) and 3'-GTAGAGGCAGGGATGATGTTC (antisense). PCR products, together with a DNA ladder as a size standard, were separated on a 1% agarose gel, stained with ethidium bromide, and quantified with the image analysis system ChemiDoc XRSn (Bio-Rad Laboratories).

### **3.5 Western blot analysis**

Immunoblotting experiments were performed according to standard procedures (43). Briefly, cells were harvested in lysis buffer (50 mM HEPES, 150 mM NaCl, 10% glycerol, 1% Triton X-100, 1 mM EGTA, 1.5 mM MgCl<sub>2</sub>, 10 mM NaF, 10 mM sodium pyrophosphate, and 1 mM Na<sub>3</sub>VO<sub>4</sub>) supplemented with a mixture of proteases and phosphatases inhibitors. Fifty micrograms of protein was electrophoresed on a 10% SDS-PAGE and transferred onto a polyvinylidene fluoride membrane. The membrane was blocked with 5% nonfat dry milk and probed with specific Abs: mouse anti-FPR1

(1  $\mu\text{g/ml}$ ), rabbit anti-FPR2 (1  $\mu\text{g/ml}$ ), mouse anti-FPR3 (1  $\mu\text{g/ml}$ ), mouse anti-uPAR R4 (1  $\mu\text{g/ml}$ ), mouse anti-uPAR<sub>84-95</sub> (1  $\mu\text{g/ml}$ ), mouse anti-Rac1 (1  $\mu\text{g/ml}$ ), mouse anti phospho-ERK (5  $\mu\text{g/ml}$ ), rabbit anti-ERK 2 (1  $\mu\text{g/ml}$ ), mouse anti-gp91<sup>phox</sup> (1  $\mu\text{g/ml}$ ), rabbit anti-p67<sup>phox</sup> (1  $\mu\text{g/ml}$ ), mouse anti-tubulin (0.5  $\mu\text{g/ml}$ ), and rabbit anti-actin (0.5  $\mu\text{g/ml}$ ). Finally, washed filters were incubated with HRP-conjugated anti-rabbit or antimouse Abs. The immunoreactive bands were detected by a chemiluminescence kit and quantified by densitometry (ChemiDoc XRS, BioRad).

### **3.6 Co-immunoprecipitation**

BJ fibroblasts ( $5 \times 10^6$  cells/sample) were plated in 100-mm dishes for 24 h. Cells were lysed in radioimmunoprecipitation assay buffer supplemented with a mixture of proteases and phosphatases inhibitors and incubated with mouse nonimmune serum (Jackson ImmunoResearch Laboratories, Suffolk, UK) and 10% protein A-conjugated Sepharose (GE Healthcare, Milan, Italy) for 2 h at 4°C. After centrifugation, the supernatants were incubated with 2  $\mu\text{g/ml}$  of the R4 monoclonal anti-uPAR Ab or with nonimmune mouse Igs for 2 h at 4°C and then with 10% protein A–Sepharose for 30 min at room temperature. The immunoprecipitates were washed in radioimmunoprecipitation assay buffer, subjected to 10% SDS-PAGE, and analyzed by Western blot analysis using a polyclonal Ab directed against FPR1.

### **3.7 Determination of ROS**

The BJ cells were plated overnight at  $2 \times 10^4$  cells/well in 96-well plates using DMEM containing 10% FBS. Cells were incubated with DCHF-DA (5  $\mu\text{M}$ ) for 30 min in the dark at 37°C; after incubation, cells were washed twice and treated with medium alone, fMLF ( $10^{-4}$  M;  $10^{-8}$  M), uPAR<sub>84-95</sub> ( $10^{-8}$  M), WKYMVm peptide ( $10^{-8}$  M), H<sub>2</sub>O<sub>2</sub> (1

mM), as a positive control, in the presence or in the absence of P25 (50 $\mu$ M), anti-uPAR<sub>84-95</sub> (5  $\mu$ g/ml), PD98059 (50  $\mu$ M), NSC23766 (25  $\mu$ M), C37 (10  $\mu$ M) and Selumetinib (2,5  $\mu$ M) for 5, 15, 30 and 60 minutes at 37°C in a humidified 5% CO<sub>2</sub> incubator. The esterified form of DCHF-DA permeate cell membranes before being deacetylated by intracellular esterases. The resulting compound, dichlorodihydrofluorescein, reacts with ROS, producing an oxidized fluorescent compound, dichlorofluorescein (DCHF), which we detected at a wavelength of 535 nm by a microplate reader (Tecan Trading AG, Switzerland).

Intracellular ROS generation by primary normal and SSc fibroblasts in a 6-well plate, after loading cells with DCHF-DA, was measured by flow cytometry (FACSCalibur). Cell monolayers were treated with medium alone, ATF-uPA (10<sup>-8</sup> M), uPAR<sub>84-95</sub> (10<sup>-9</sup> M), WKYMVm peptide (10<sup>-9</sup> M), or H<sub>2</sub>O<sub>2</sub> (1 mM), as a positive control, for 30 min at 37°C in a humidified 5% CO<sub>2</sub> incubator. Cells were then washed twice, and 5  $\mu$ M DCHF-DA was added for 30 min in the dark at 37°C. After incubation, cells were washed, trypsinized for immediate analysis, and resuspended in PBS. A total of 10<sup>4</sup> events were acquired for each sample in all cytofluorimetric analysis, and intracellular ROS formation was detected as a result of the oxidation of DCHF which can be detected by flow cytometry at a wavelength of 520 nm (FL1). Results are expressed as percentage of increase of mean fluorescence intensity in respect to untreated cells.

### **3.8 Flow cytometric analysis of surface molecules**

Flow cytometric analysis of cell surface molecules was performed as previously described (43). Briefly, after saturation of non specific binding sites with total rabbit IgG, cells were incubated for 20 min at +4°C with specific or isotype control antibodies. For indirect staining this step was followed by a second incubation for 20 min at +4°C

with an appropriate anti-isotype-conjugated antibody. Finally, cells were washed and analyzed with a FACSCalibur Cytofluorometer using Cell Quest software (Becton & Dickinson, San Fernando, CA). A total of  $10^4$  events for each sample were acquired in all cytofluorimetric analyses.

### **3.9 Determination of Rac1 activity and association with p67<sup>phox</sup>**

The BJ cell line was incubated at 37°C with or without specific agonists for the indicated times, washed with phosphate-buffered saline, and then lysed in MLB buffer (10µg/mL aprotinin and 10 µg/mL leupeptin) in the presence of protease and phosphatase inhibitors. After being centrifuged at  $12,000 \times g$  for 5 min at 4°C, the same amount of total protein from clarified lysate was incubated with GST-PBD (p21-binding domain of human PAK-1) to precipitate GTP-bound Rac1 at 4°C on a rotator for 1 h and then the beads were pelleted through centrifugation at  $14,000 \times g$  for 10 seconds at 4°C. The resulting pellet was resuspended in Laemmli buffer, boiled for 5 min and subjected to Western blot analysis with anti-Rac1 Ab or with anti p67<sup>phox</sup> Ab. Total Rac1 and p67<sup>phox</sup> in each sample was also determined, as a loading control.

### **3.10 Histology and immunohistochemistry**

After clinical evaluation, a 3-mm skin punch was taken from the most representative area of each patient affected by SSc and from 10 normal subjects as a control. Each specimen was fixed in 10% buffered formalin, embedded in paraffin, and serial sectioned (4-mm-thick sections). One section for each case was stained with H&E and the others stained by immunohistochemistry (labeled streptavidin biotin standard technique) with specific antibodies. Cells showing a definite black staining confined to the nucleus or cytoplasm were judged positive. All slides were examined in a double-

blinded fashion by two investigators, and the final staining for each case was expressed as the percentage of positive cells among the total number of counted cells (at least five high-power representative fields).

### **3.11 Statistical analysis**

All the experiments were performed at least in triplicate. The results are expressed as mean  $\pm$  SEM. Values from groups were compared using a paired Student t test (49). Differences were considered significant when  $p < 0.05$ .

## **4. RESULTS**

### ***4.1 In vivo expression of FPR1, FPR2, and FPR3 in human normal and SSc skin fibroblasts***

*N*-formyl peptide receptors (FPRs), a family of pattern recognition receptors, possess important regulatory effects in multiple pathological conditions, including inflammation and cancer.

To test the possibility that FPRs are involved in the pathogenesis of SSc, we investigated whether they were expressed on fibroblasts from skin punch biopsies of 10 patients affected by SSc and of 10 normal subjects, as a control. At histological analysis, (H&E staining, in Fig. 5A a representative case), all enrolled SSc cases (six limited cutaneous and four diffuse cutaneous) showed dermal fibrosis that characteristically involved the subcutis, associated with chronic inflammatory infiltrate, mainly localized at the interface between the deep dermis and subcutis and around vessels (a–c), as compared with normal skin (d). All the evaluated cases showed an increased positivity for FPR1 (e–g), FPR2 (i–k), and FPR3 (m–o), compared with that observed in normal skin (h, l, p), used as a control.

FPR1 was found diffusely positive in fibroblasts, endothelial cells, and lymphocytes. FPR2 was expressed in several but not all fibroblasts, whereas FPR3 was seen extensively expressed only in fibroblasts.

### ***4.2 In vitro expression of FPR1, FPR2, and FPR3 in human normal and SSc skin fibroblasts***

We also examined FPRs expression in primary cultures of skin fibroblasts from 10 normal subjects and 10 SSc patients. The analysis of total RNA by RT-PCR showed expression of all three FPRs (Fig. 5B), that resulted upregulated in SSc fibroblasts as

compared with normal fibroblasts, with a significant increase for FPR2 and FPR3 (fold increase SSc versus normal fibroblasts: FPR1 2.6; FPR2 5.17; and FPR3 6.08) (Fig. 5B).

We then investigated FPRs expression in normal and SSc fibroblasts at a protein level. Western blot analysis with specific antibodies demonstrated that fibroblasts synthesize all the three FPRs (Fig. 5C). Unexpectedly, we observed a different pattern of increase of FPR protein expression as compared with mRNA levels. Indeed, FPR1 and FPR3 expression increased in SSc fibroblasts as compared with normal fibroblasts (fold increase SSc versus normal fibroblasts: FPR1 4.07; FPR3 1.3;  $p < 0.05$ ), whereas FPR2 was not significantly upregulated (fold increase SSc versus normal fibroblasts 1.02) (Fig. 5C).

These experiments demonstrate that both normal and SSc fibroblasts express FPRs; moreover, SSc fibroblasts show an overexpression as compared with normal cells. It is conceivable that posttranscriptional mechanisms may regulate the expression of these receptors in normal and SSc fibroblasts, causing a different expression pattern at mRNA and protein level. The histology data are in agreement with the *in vitro* observations, showing a lower expression of FPR2, at a protein level, in SSc fibroblasts, compared with FPR1 and FPR3.

#### ***4.3 In vivo and in vitro expression of uPAR forms in human foreskin fibroblasts***

Several functions of FPRs occur through the interaction with the urokinase-type plasminogen activator (uPA) receptor (uPAR) (41).

uPAR cleavage contributes to the impaired angiogenesis observed in SSc patients (50). Inactivation of uPAR gene induces dermal and pulmonary fibrosis and peripheral microvasculopathy in mice. Moreover, native full-length uPAR expression is

significantly decreased in the skin of SSc patients, as assessed by a monoclonal anti-uPAR/domain DI antibody (51).

Thus, although full-length uPAR expression is significantly downregulated in SSc dermis, we hypothesized that the DII-DIII-uPAR<sub>88-92</sub> form, able to interact with FPRs, could instead be increased. To confirm our hypothesis, we investigated the expression of the different uPAR forms in SSc skin biopsies, by immunohistochemistry with specific antibodies. In particular, we used the R3 monoclonal antibody, which recognizes domain DI (52), the IB polyclonal antibody, specifically directed against the <sup>88</sup>Ser-Arg-Ser-Arg-Tyr<sup>92</sup> sequence of uPAR (53), and the ADG3937 monoclonal antibody, recognizing an epitope located in the domains DII+DIII.

SSc skin biopsies revealed dermal fibrosis showing prominent involvement of the deep dermis and the subcutaneous fat, admixed with chronic inflammatory infiltrate, mostly confined deeply around vessels of the subcutis. As expected, all biopsies showed an absent/low staining for R3, in fibroblasts, endothelial cells and lymphocytes. Conversely, IB was found positive in fibroblasts, endothelial cells and lymphocytes of all specimens; finally, ADG3937 was expressed only in 4 out 14 selected cases (Fig. 6A).

In Figure 6B is reported a staining for IB on a skin biopsy of localized scleroderma previously evaluated for FPR1, FPR2 and FPR3 expression: fibroblasts, lymphocytes and endothelial cells were strongly positive for IB, as reported for FPRs antibodies (see Fig. 5A).

We also investigated DII-DIII-uPAR<sub>88-92</sub> expression in primary cultures of normal and SSc fibroblasts by Western blot analysis, using the polyclonal IB antibody. Figure 6C shows that SSc fibroblasts markedly overexpressed DII-DIII-uPAR<sub>88-92</sub> (fold increase SSc fibroblasts versus normal cells: 4.7;  $p < 0.05$ ).

Thus, in SSc fibroblasts, full length uPAR down-regulation, most probably due to the induction of the uPA pathway (47), is accompanied by increased membrane expression of DII-DIII-uPAR<sub>88-92</sub>, containing the chemotactic sequence able to interact with overexpressed FPRs.

#### ***4.4 Expression of FPRs in human normal fibroblasts; uPAR expression and direct interaction with FPR1 in human normal foreskin fibroblasts***

In order to further study FPRs functions and their possible cross-talk with uPAR in fibroblast cells, we sought a fibroblast cell line to be used as a model.

We first investigated, by cytofluorimetric analysis, FPRs expression in three human fibroblast cell lines from different sources: normal foreskin fibroblasts (BJ cells), normal gingival fibroblasts (HGF-1 cells), and normal lung fibroblasts (MRC5 cells). Normal fibroblasts from the three cell lines, even with a different pattern of expression, synthesized all the three members of the FPRs family (Fig. 7A).

Thus, for subsequent studies on FPRs functions, we focused on the BJ fibroblast cell line. BJ fibroblast cells were established from normal human foreskin and have the ability to proliferate to a maximum of 72 population doublings before the onset of senescence (54).

BJ fibroblasts, tested at different times of culture, expressed both forms of uPAR, but mostly the native intact form, thus confirming *in vivo* observations (51) (Fig. 7B).

Since both intact and cleaved DII-DIII-uPAR<sub>88-92</sub>(55), either on the cell membrane (56) or in a soluble form (44) can interact with FPRs, in many cell types (33), to investigate whether such interaction could also occur in normal fibroblast cells, a pull-down experiment was carried out in human skin fibroblasts from the BJ cell line.

In BJ cells, immunoprecipitation with a monoclonal anti-uPAR antibody and Western blot analysis of the immunoprecipitate with polyclonal anti-FPR1 antibodies revealed a band corresponding to FPR1 that was absent in the same lysate immunoprecipitated with nonimmune Igs. As a control, a corresponding band was evidenced in BJ total cell lysates subjected to Western blot analysis with anti-FPR1 antibodies (Fig. 7C).

Therefore, a structural interaction between uPAR and FPR1 can occur in normal fibroblast cells and exert functional effects.

#### ***4.5 Effects of fMLF, WKYMVm peptide, and uPAR<sub>84-95</sub> on ROS production in human normal foreskin fibroblasts***

We have already demonstrated that FPRs stimulation promotes  $\alpha$ -smooth muscle actin expression in primary cultures of normal dermal fibroblasts as well as motility, matrix deposition, and  $\alpha\text{v}\beta 5$  integrin expression, thus playing a role in fibrosis and in the fibroblast-to-myofibroblast transition (57).

In this thesis, we sought to investigate whether FPRs stimulation and their cross-talk with uPAR could induce radical oxygen species (ROS) generation in fibroblast cells, thus playing a role in some processes involved in SSc, such as tissue remodeling and fibrosis.

It is well established that low/moderate concentrations of ROS are involved in the redox-dependent regulation of multiple signal transduction pathways and in essential biological processes, including cell adhesion, migration, proliferation, differentiation, and survival (58, 59). However, at high levels, ROS are known to exert very damaging effects through oxidative stress. This is caused by an imbalance between the ROS production and the ability of cellular antioxidant mechanisms to detoxify the reactive intermediates, thus amplifying the risk of cellular dysfunction and oxidative injury (58).

There are accumulating evidences suggesting a role of the oxidative stress in the pathogenesis of SSc (1); indeed, it has been shown that ROS contribute to the persistent fibrotic phenotype of SSc fibroblasts (10) and that antioxidants, such as epigallocatechin-3gallate, can reduce ECM production, function, and activity of dermal fibroblasts from SSc patients (11).

Several studies have described, among the various properties of FPRs, the capability to induce ROS generation upon binding to their specific ligands (60). Interestingly, SSc neutrophils may induce local production of ROS upon fMLF stimulation in endothelium (60).

On these basis, we investigated the effects of FPRs activation and cross-talk with uPAR on ROS release from normal fibroblasts, using the BJ cell line as a model.

To this aim, we evaluated ROS levels after stimulation with specific FPRs agonists, such as fMLF, the synthetic peptide WKYMVm, and the soluble uPAR<sub>84-95</sub> peptide, containing the uPAR-derived <sup>88</sup>SRSRY<sup>92</sup> sequence, able to bind and activate FPRs. The intracellular ROS levels were determined after 5, 15, 30, and 60 minutes of stimulation with fMLF, WKYMVm peptide, and uPAR<sub>84-95</sub>, and compared with unstimulated cells. As shown in Figure 8, dermal fibroblasts from the BJ cell line responded in a significant manner to all the three stimuli ( $p < 0.05$ ), thus suggesting that FPRs stimulation could be involved in ROS production in normal fibroblast cells as well as their cross-talk with uPAR, through the <sup>88</sup>SRSRY<sup>92</sup> sequence.

#### ***4.6 FPRs-uPAR-Integrin crosstalk as a potential player in ROS generation by human normal foreskin fibroblasts***

uPAR is an important signaling partner of FPRs at the cell-surface. Moreover, a large body of evidence shows that uPAR also requires integrins as co-receptors. In tumor

cells, uPAR overexpression controls the mechanisms of cell migration and invasion by recruiting integrins and FPR1 at the cell surface and regulating their signaling pathways (55). Thus, we hypothesized that FPRs could regulate ROS production in fibroblast cells through the same mechanism.

To test our hypothesis, ROS production assay was performed in the presence of IB, a polyclonal antibody directed against the uPAR<sub>88-92</sub> region involved in uPAR interaction with FPRs (44) and in the presence of the P25 peptide, which has been shown to disrupt uPAR interactions with  $\beta$ 1 or  $\beta$ 2 integrins (61).

Figure 9 shows that treatment of BJ cells with the IB antibody and the P25 peptide totally inhibited FPRs-mediated ROS production, in response to their specific agonists, fMLF and the WKYWM peptide. Non immune antibodies and a scrambled peptide, used as controls, did not exert any effect.

These results suggest that FPRs could control ROS production by interacting with uPAR and forming a complex with integrins, as already demonstrated for cell migration and invasion (55).

#### ***4.7 Rac1 and ERK1/2 pathways are involved in ROS production after FPRs stimulation in human normal foreskin fibroblasts***

In order to study the signaling pathways involved in FPRs mediated ROS generation in fibroblast cells, we focused our attention on the small GTPase Rac1 and on the ERK1/2 pathway.

Indeed, uPAR-controlled cell migration, which is allowed by uPAR interactions with FPRs and  $\beta$ 1 integrins, involves specifically small Rac1 and Rho GTPases as signaling mediators (55). Moreover, one important effector of Rac1 activity is p67<sup>phox</sup>, which combines with other components of the NADPH oxidase system to generate a functional complex for producing ROS (62).

NADPH oxidase system-derived ROS can also activate other downstream signals, such as ERK 1/2 signalling pathways (63). Moreover, uPAR-dependent signaling pathways can also include PI3K and lead to the activation of ERK MAPKs (38).

Thus, we analyzed the effects of FPRs stimulation with fMLF, WKYMVm peptide, and uPAR<sub>84-95</sub> on Rac1 and ERK1/2 activation. All the stimuli, even with different kinetics, increased the levels of Rac1-GTP and p-ERK 1/2 (Fig. 10).

Furthermore, we evaluated ROS levels after stimulation with the same agonists, in the absence and the in presence of an inhibitor of Rac-specific GEF (guanine nucleotide exchange factor) Trio and Tiam1 (NSC23766) and of a specific MEK 1/2 inhibitor (PD98059). BJ cells, which responded in a significant manner to all the three stimuli ( $p < 0.05$ ), were incapable to produce ROS in presence of NSC23766 and PD98059 (Fig. 11).

These data suggest that FPRs stimulation in normal fibroblasts could determine ROS production by activating Rac1 and ERK 1/2 dependent signals.

#### ***4.8 FPRs induce ROS production through the upregulation and activation of NADPH oxidase-2 in human normal foreskin fibroblasts***

After establishing that FPRs activation induced ROS production through Rac1 and ERK 1/2 signaling in the BJ cell line, we investigated whether ROS were generated by the NADPH oxidase-2 (Nox2 complex), being this NADPH oxidase isoform expressed in fibroblasts and mainly involved in SSc pathogenesis (64).

Upon stimulation, activated GTP bound-Rac1 and/or Rac2 translocate to the plasma membrane and recruits p67<sup>phox</sup> by binding to its N-terminal. The binding of p67<sup>phox</sup> to Rac1/2-GTP is the limiting step in the assembly of the active NADPH oxidase complex (62).

To investigate whether FPRs stimulation could induce ROS production through upregulation and/or activation of the Nox2 complex, we evaluated, by Western Blot analysis, the expression levels of gp91<sup>phox</sup> and p67<sup>phox</sup> after stimulation with specific agonists of FPRs. As shown in Figure 12, BJ cells responded in a significant manner to all the stimuli by upregulating the expression of both gp91<sup>phox</sup> and p67<sup>phox</sup>.

Rac1-GTP, but not Rac1-GDP, directly interacts with the N-terminal tetratricopeptide repeat (TPR) domain of p67<sup>phox</sup> (29, 30), and serves as an “adaptor” by providing a stable platform for the interaction with the catalytic component gp91<sup>phox</sup>.

To investigate whether FPRs stimulation could induce the interaction between Rac1-GTP and p67<sup>phox</sup>, a pull-down experiment was carried out in BJ cells, after stimulation with specific FPRs agonists. Active Rac1 (Rac1-GTP) was precipitated from cell lysates using the p21-binding domain (PBD) of its target, PAK1, bound to agarose beads. Rac1-GTP was eluted from beads and Western blot analysis of the precipitate with a polyclonal anti-p67<sup>phox</sup> antibody revealed that FPRs stimulation increased interaction between Rac1-GTP and p67<sup>phox</sup>, thus allowing the assembly of the active Nox2 complex (Fig.13).

After stimulation with specific FPRs agonists, no increased association between Rac1-GTP and gp91<sup>phox</sup> could be detected (not showed).

Thus, our data demonstrated that FPRs/uPAR-mediated ROS generation in fibroblast cells is mediated by a direct binding of Rac1 to p67<sup>phox</sup> that, in turn, interacts with the gp91<sup>phox</sup> and p22<sup>phox</sup> membrane subunits to generate the active Nox2 complex.

#### ***4.9 FPRs mediated ROS production in human normal and SSc skin fibroblasts***

In a next series of experiments, we also studied ROS release in primary cultures of normal and SSc fibroblasts.

First, normal and SSc fibroblasts were tested, by flow cytometry analysis, for the ability to induce ROS generation. The basal level of fluorescence was determined in both cell types after loading with DCHF-DA. DCHF-DA-loaded normal and SSc fibroblasts didn't show a different level of basal ROS production (Fig. 14A). After cell stimulation with H<sub>2</sub>O<sub>2</sub> (1 mM), normal and SSc fibroblasts showed a similar, significant increase in ROS production (Fig. 14B).

To prove that FPRs stimulation may have a role in ROS production also in primary fibroblasts, we evaluated ROS levels after 30 min of stimulation with the aminoterminal fragment of uPA (ATF-uPA), able to unmask the <sup>88</sup>SRSRY<sup>92</sup> sequence upon binding intact uPAR, the soluble uPAR<sub>84-95</sub> peptide, and the FPRs agonist WKYMVm peptide and compared them with unstimulated cells. As shown in Figure 14C, normal primary skin fibroblasts responded in a significant manner to all the three stimuli ( $p < 0.05$ ), whereas in SSc fibroblasts, only the WKYMVm peptide significantly induced ROS generation.

Thus, FPRs stimulation is effective in ROS production both in normal and SSc skin fibroblast; the response to ATF and uPAR<sub>84-95</sub> is downregulated in SSc fibroblasts as compared to normal.

#### ***4.10 Therapeutic strategies to modulate FPRs/uPAR-mediated generation of oxidative stress by fibroblast cells***

We demonstrated FPRs involvement in ROS production and in the generation of oxidative stress, playing a key role in pathogenesis of fibrosis.

Thus, we sought to investigate whether inhibition of the structural and functional interaction between FPRs and uPAR could affect ROS generation in BJ cell line. After stimulation with fMLF and the WKYMVm peptide, we treated cells with C37, a new

small molecule identified by our group through structure-based virtual screening, and able to inhibit uPAR and FPRs cross-talk by targeting the <sup>88</sup>SRSRY<sup>92</sup> sequence of uPAR, in the hot-spot residue Arg<sup>91</sup> (65). Figure 15A shows that the BJ cells, which responded in a significant manner to both stimuli ( $p < 0.05$ ), were incapable to produce ROS in presence of C37.

Many studies have shown that MAPKs are activated in response to fibrogenic agents and contribute to the formation and function of the myofibroblast, the critical cell type responsible for excessive scarring. Recently it has been demonstrated that the specific MEK inhibitor ARRY-142886 can both suppress the progression of fibrosis and reverse an animal model of lung fibrosis. Thus, MEK inhibition could be a valuable method to treat lung fibrosis (66). Moreover, we have demonstrated ERK 1/2 involvement in ROS generation induced by FPRs/ uPAR activation.

Therefore, we investigated the effects of Selumetinib, a highly selective MEK1 inhibitor currently approved for various anticancer therapies, on ROS release mediated by FPRs/uPAR activation. As shown in Figure 15B, Selumetinib completely abolished ROS production, in response to FPRs/uPAR specific agonists in BJ cell line.

Results from these studies show that C37 and Selumetinib, through inhibition of FPRs-mediated ROS generation, may lead to the development of novel antifibrotic therapeutic strategies.

## 5. CONCLUSIONS

*N*-formyl peptide receptors (FPRs) are a family of pattern recognition receptors, regulating innate responses. FPRs, by interacting with several structurally diverse pro- and anti-inflammatory ligands, possess important regulatory effects in multiple pathophysiological conditions, including inflammation and cancer.

Three variants of FPRs have been identified in humans: FPR1, FPR2, and FPR3. FPR1 is activated by nanomolar concentrations of fMLF. FPR2 is a promiscuous receptor activated in response to high concentrations of fMLF, and to viral, bacterial, endogenous and synthetic peptides. Hp(2-20), uPAR<sub>84-95</sub>, and F2L are natural ligands of FPR3. The synthetic peptide WKYVM is mainly a FPR2 and FPR3 agonist (18).

Several functions of FPRs occur through the interaction with the urokinase-type plasminogen activator (uPA) receptor (uPAR). uPAR is formed by three homologous domains (DI, DII, DIII) anchored to the cell surface by a glycosyl-phosphatidylinositol (GPI) tail and is able to interact with integrins, FPRs and tyrosine kinase receptors, representing a main regulator of signal transduction pathways involved in wound repair, tumor progression and angiogenesis (55). A specific region of uPAR, corresponding to amino acids 88-92 (SRSRY), located in the flexible linker connecting uPAR domains DI and DII, is able to interact with FPRs, mediating uPA or fMLF-dependent cell migration. uPA or its aminoterminal fragment (ATF) can promote uPAR interaction with FPRs, by determining the exposure of the uPAR<sub>88-92</sub> region, upon binding to the receptor. Further, uPA-mediated removal of DI results in the membrane expression of a truncated uPAR form, that can contain the chemotactic peptide able to interact with FPRs and to regulate their signal (DII-DIII-uPAR<sub>88-92</sub>) (37).

Recently, to test the possibility of FPRs being involved in the pathogenesis of SSc, we have demonstrated that FPRs stimulation promotes  $\alpha$ -smooth muscle actin expression in

primary cultures of normal dermal fibroblasts as well as motility, matrix deposition, and  $\alpha\beta 5$  integrin expression, thus playing a role in fibrosis and in the fibroblast-to-myofibroblast transition (57).

In this thesis, we investigated whether FPRs stimulation and their cross-talk with uPAR could induce radical oxygen species (ROS) generation, thus playing a role in some ROS-mediated processes involved in SSc, such as tissue remodeling and fibrosis.

We provided evidence, for the first time, that FPRs are expressed by human normal skin fibroblasts and that SSc fibroblasts overexpress these receptors both *in vitro* and *in vivo*. Furthermore, SSc fibroblasts showed increased membrane expression levels of DII-DIII-uPAR<sub>88-92</sub>, expressing at the N-terminus the chemotactic sequence able to interact with overexpressed FPRs. Induction of the uPA pathway could be responsible for the increased expression of this cleaved uPAR form (67) even though our group could observe uPA increase only in localized SSc forms (47).

In order to study the molecular mechanisms of FPRs-mediated ROS generation in fibroblast cells, we pursued our studies on the BJ cell line. We demonstrated that FPRs stimulation induced ROS generation in normal fibroblasts by interacting with uPAR and forming a complex with integrins, as already demonstrated in epithelial cell migration and invasion (34). Our study also reported that FPRs/uPAR/ $\beta 1$  integrin cross-talk determines ROS production through Rac1 and ERKs activation in human skin fibroblasts.

One important effector of Rac1 activity is p67<sup>phox</sup>, which combines with the NADPH oxidase system to generate a functional complex for producing ROS. Upon activation by GTP-Rac1, p67<sup>phox</sup> translocates to the membrane where it associates with gp91<sup>phox</sup>. FPRs stimulation promoted gp91<sup>phox</sup> and p67<sup>phox</sup> expression as well as a direct interaction between GTP-Rac1 and p67<sup>phox</sup>.

We finally analyzed the effects of FPRs and uPAR stimulation on ROS production in normal and SSc fibroblasts from primary cultures. The intracellular ROS levels were determined after stimulation with ATF-uPA, able to bind only intact three domain uPAR, the soluble uPAR<sub>84-95</sub> peptide, containing the uPAR-derived <sup>88</sup>SRSRY<sup>92</sup> sequence, able to bind and activate FPRs, and the WKYMVm peptide, mostly acting on FPR2 and FPR3. Normal fibroblasts significantly responded to all the agonists, thus confirming that stimulation of FPRs and their crosstalk with uPAR could be involved in ROS production also in primary cells; on the contrary, only the WKYMVm peptide was a potent stimulus for SSc fibroblasts. As expected from histology, the absence of response to ATF-uPA in SSc fibroblast is not surprising; indeed, they do not express intact uPAR. The difference in the effect between uPAR<sub>84-95</sub> and WKYMVm peptides could be due to the preferential involvement of FPR3 in the cross-talk with uPAR in SSc fibroblasts. Indeed, FPR3 is exquisitely overexpressed in SSc fibroblasts, in respect to normal (Fig. 5) and the WKYMVm peptide is mostly a FPR2 and FPR3 agonists.

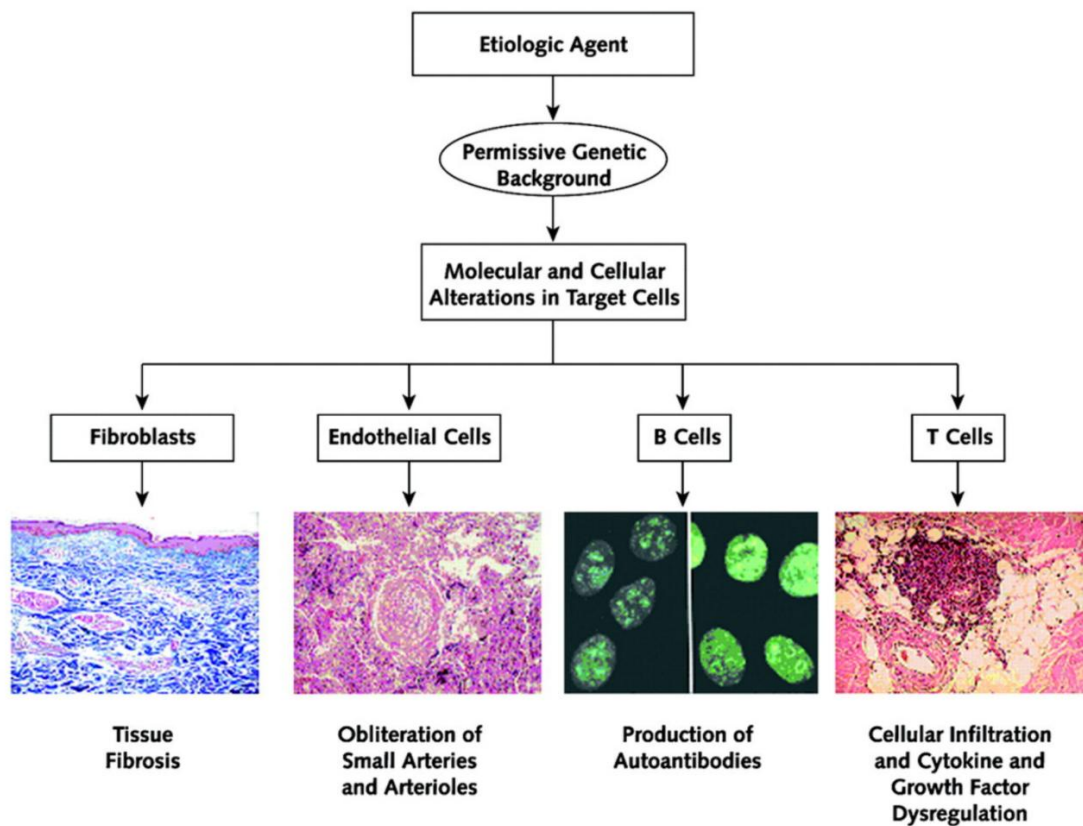
In SSc fibroblasts, membrane overexpressed DII-DIII-uPAR<sub>88-92</sub> could mostly interact with FPR1, and desensitize it toward uPAR<sub>84-95</sub>.

However, FPRs, through the interaction with the uPA/uPAR system, are responsible for ROS production both in normal and SSc fibroblasts, making them a potential novel therapeutic target in the treatment of SSc. Indeed, the treatment with C37, able to inhibit the cross-talk between FPRs and uPAR, and the inhibition of the MAPK/ERK pathway with Selumetinib, inhibited ROS production, after stimulation of FPRs with specific ligands.

In conclusions, the results of the present study show that the FPRs, through the interaction with the uPA/uPAR system, induce increased levels of ROS, thereby contributing to the scleroderma phenotype. In particular, the FPRs derived signals and

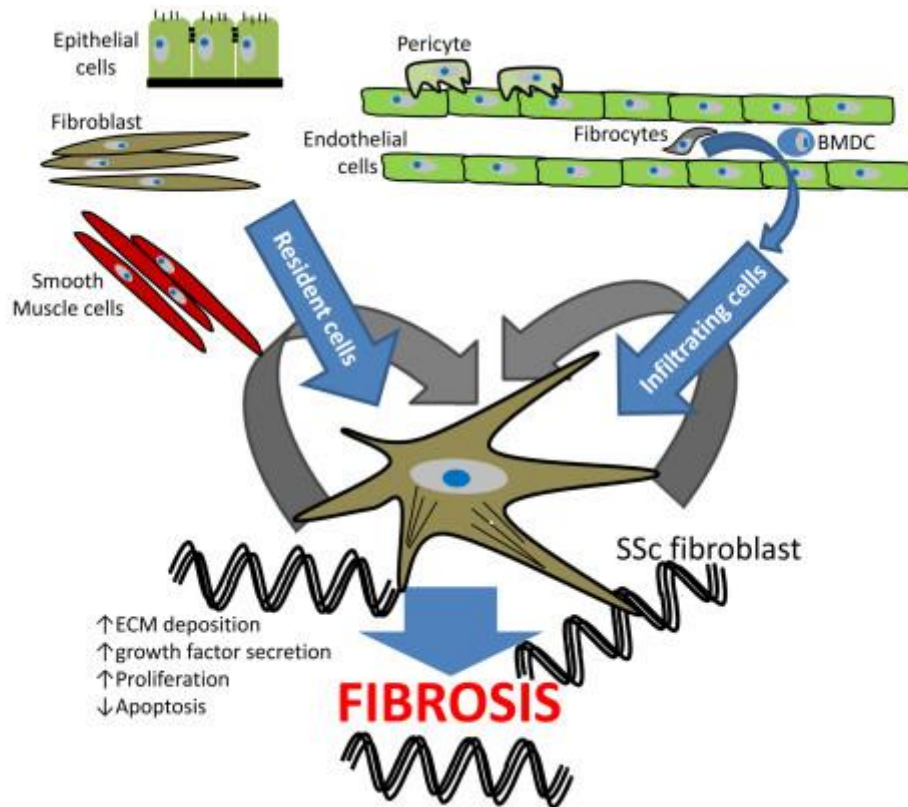
their cross-talk with uPAR appears to be important both in normal and SSc fibroblasts. Since, in SSc, early recognition and treatment of symptoms and life-threatening complications are crucial for patient clinical evolution, these observations can help in the development of novel therapeutic target in the treatment of early SSc.

## 6. FIGURES



*Jimenez, S. A. et al. Ann Intern Med, 2004.*

**Figure 1. General overview of the pathogenesis of systemic sclerosis.** The pathogenesis of SSc is extremely complex and remains incompletely understood. At present, no single unifying hypothesis explains all aspects of its pathogenesis. However, fundamental abnormalities in at least 3 types of cells are involved in the development of the clinical and pathologic manifestations of the disease: 1) fibroblasts; 2) endothelial cells; 3) immune cells, particularly T and B lymphocytes. The illustrations show examples of, from left to right, the fibrotic process (biopsy of skin), microvascular alterations in pulmonary arterioles, autoantibodies detected by immunofluorescence, and mononuclear inflammatory cell infiltrates in affected skin.



*Gilbane, A. J. et al. Arthritis Res Ther, 2013.*

**Figure 2. The cellular origins of pathogenic “activated” fibroblasts in scleroderma.** Myofibroblast, the mesenchymal cell type most responsible for the excessive matrix production and deposition in tissue and vessel wall, found in fibrotic disorders and fibroproliferative vasculopathies. In fibrotic diseases, myofibroblasts may derive from at least three sources: 1) expansion and activation of resident tissue fibroblasts; 2) transition of epithelial cells into mesenchymal cells, a process known as epithelial–mesenchymal transition; and 3) tissue migration of bone marrow–derived circulating and fibrocytes. SSc fibroblasts also promote a pro-fibrotic microenvironment, secreting growth factors, chemokines and cytokines that can in turn act on resident and infiltrating cells in an autocrine and paracrine manner to expand the reservoir of pro-fibrotic fibroblasts present in SSc fibrotic lesions.

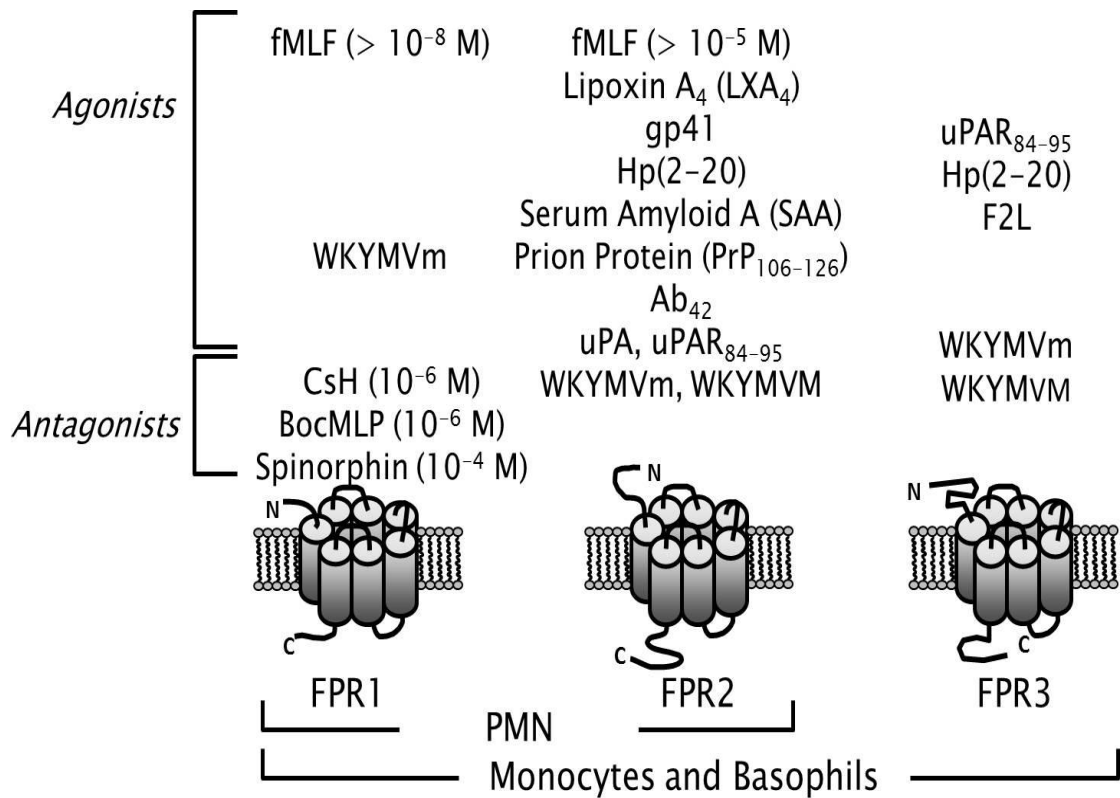


**Figure 3. Agonists and antagonists of the *N*-formyl peptide receptor family.** The family of *N*-formyl peptide receptors (FPRs) consists of three members defined: FPR1, FPR2 and FR3, that share a high degree of sequence homology. These receptors are capable of binding a very large number of ligands with different structural characteristics, including peptides formylated and not formylated, that, by acting as agonists, determine their activation. Upon agonist binding, FPRs are subjected to inactivation by desensitization.

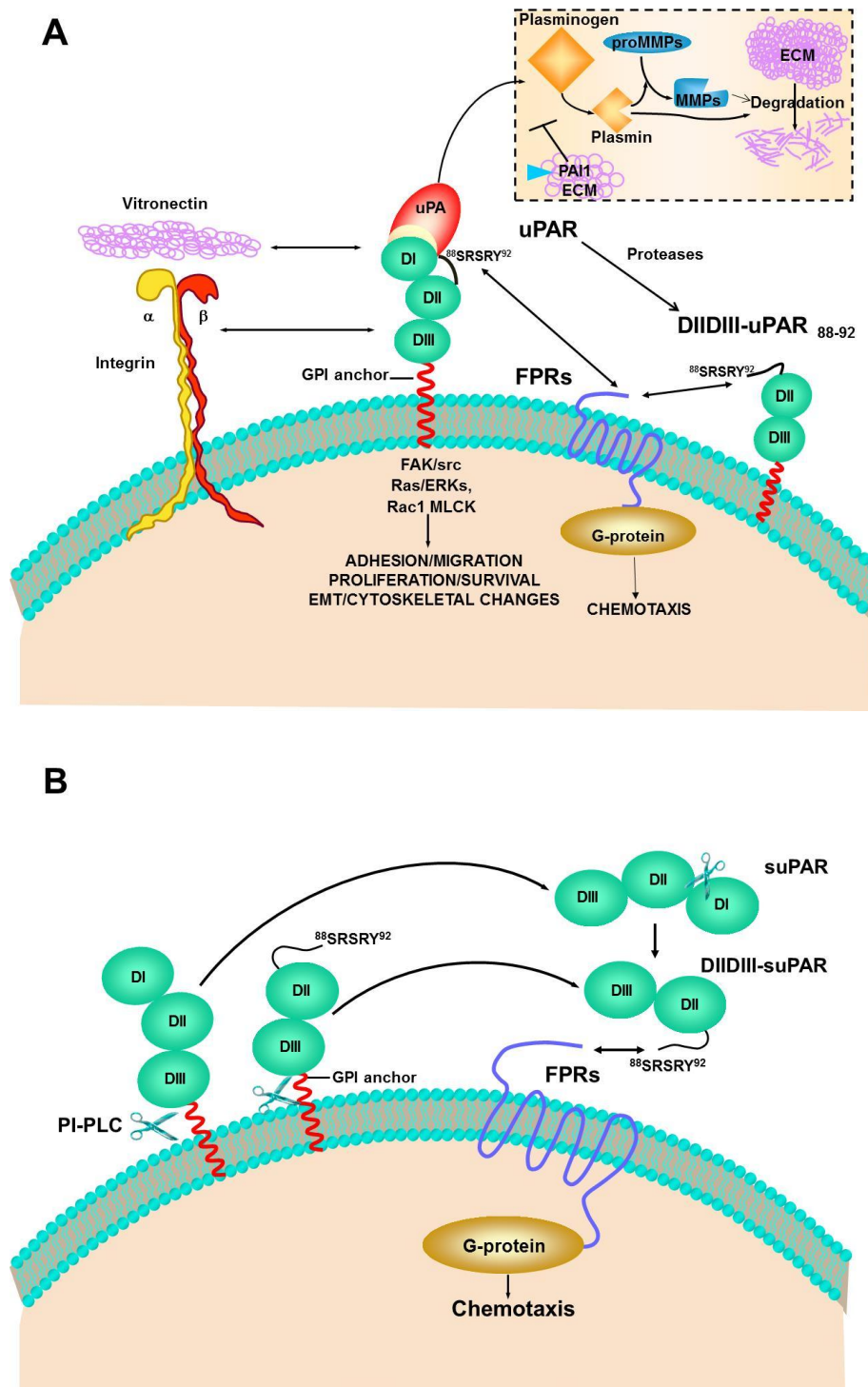


**Figure 4. Urokinase-type plasminogen activator (uPA) receptor (uPAR) forms and activities.**

**A:** plasma membrane uPAR is a GPI-anchored protein that binds with high-affinity the serine protease uPA, thus focusing its proteolytic activity at the cell surface. In addition, uPAR is an adhesion receptor and binds vitronectin (VN), a component of provisional ECM. Upon uPA and/or VN binding, uPAR interacts with the integrin family of adhesion receptors, thus regulating cell adhesion, proliferation and migration. Upon uPA binding or proteolytic cleavage, uPAR or its truncated form (DIIDIII-uPAR<sub>88-92</sub>) interacts with FPRs through the <sup>88</sup>SRSRY<sup>92</sup> sequence. uPAR/FPRs interaction is necessary for both uPAR and FPRs-mediated chemotaxis.

**B:** phosphatidyl-inositol specific phospholipases can cleave the GPI anchor of uPAR thus releasing from the cell surface soluble uPAR forms that have been detected in human plasma and urine. Soluble intact uPAR (suPAR) retains all the activities of membrane-bound uPAR; the cleaved soluble form of uPAR (DIIDIII-suPAR<sub>88-92</sub>) is only able to bind FPRs through the <sup>88</sup>SRSRY<sup>92</sup> sequence.

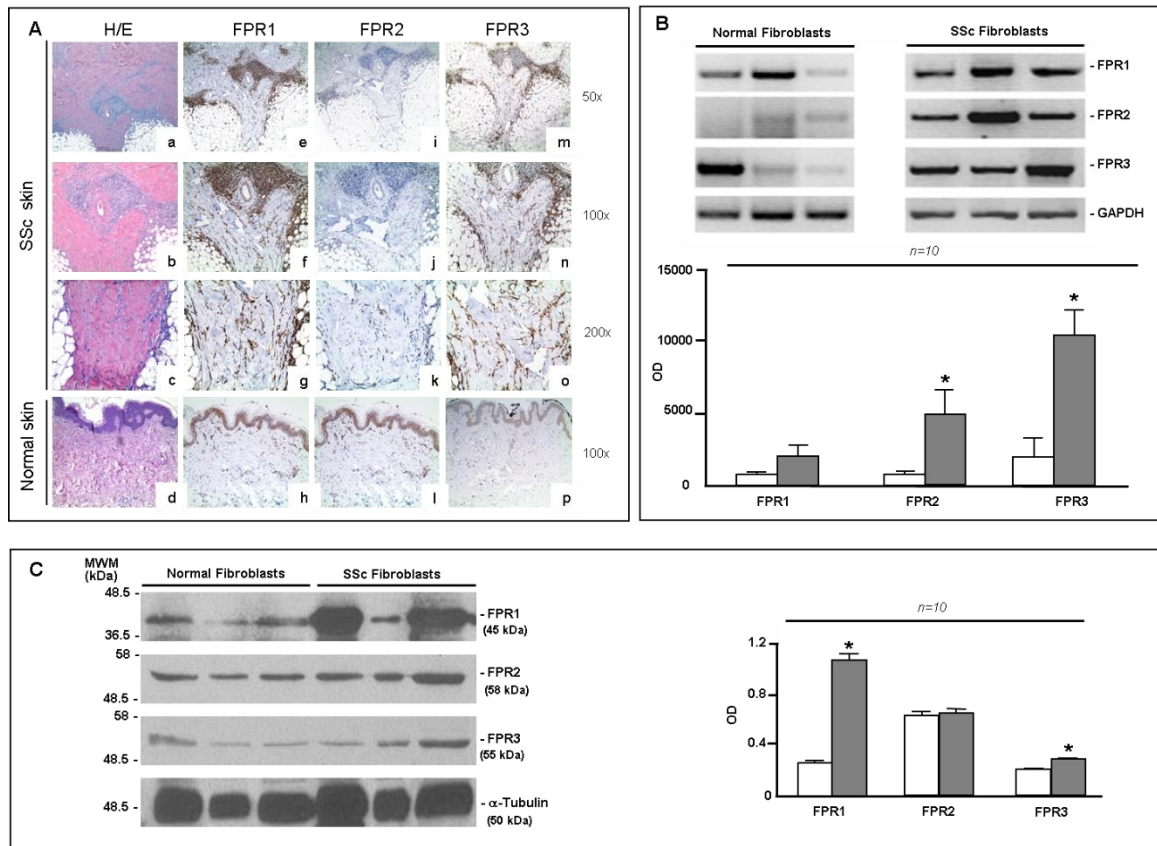


**Figure 5. FPRs expression in normal and SSc skin fibroblasts.**

**A:** Histological expression of FPRs in skin biopsies. (a–c) Histologic appearance of a localized scleroderma. (d) Histologic appearance of normal skin. (e–g) Immunostaining for FPR1 in a localized scleroderma. Overexpression of FPR1 was observed in fibroblasts, endothelial cells, and lymphocytes. (h) Immunostaining for FPR1 in normal skin. Weak expression of FPR1 was observed in fibroblasts, lymphocytes, and endothelial cells. (i–k) Immunostaining for FPR2 in a localized scleroderma. Only a minority of fibroblasts resulted positive for FPR2. (l) Immunostaining for FPR2 in normal breast skin in normal skin. Only two fibroblasts resulted positive for FPR2. (m–o) Immunostaining for FPR3 in a localized scleroderma. Most fibroblasts show positivity for FPR3. Lymphocytes and endothelial cells were negative. (p) Immunostaining for FPR3. Some fibroblasts showed positivity for FPR3. Lymphocytes and endothelial cells were negative.

**B:** mRNA expression of FPRs in normal and SSc fibroblasts with FPR1, FPR2, and FPR3-specific primers and GAPDH primers as loading control. Densitometric analysis of the FPR expression in normal (white columns) and SSc (gray columns) fibroblasts show that SSc fibroblasts overexpress FPR2 and FPR3 as compared with normal fibroblasts.

**C:** Western blot analysis of FPRs in normal and SSc fibroblasts with anti-FPR1, anti-FPR2, and anti-FPR3 specific Abs and then with  $\alpha$ -tubulin Ab for loading control. Normalization with  $\alpha$ -tubulin using densitometric analysis of the FPR protein levels shows a significant increase of FPR1 and FPR3 in SSc fibroblasts (gray columns) as compared with normal fibroblasts (white columns).

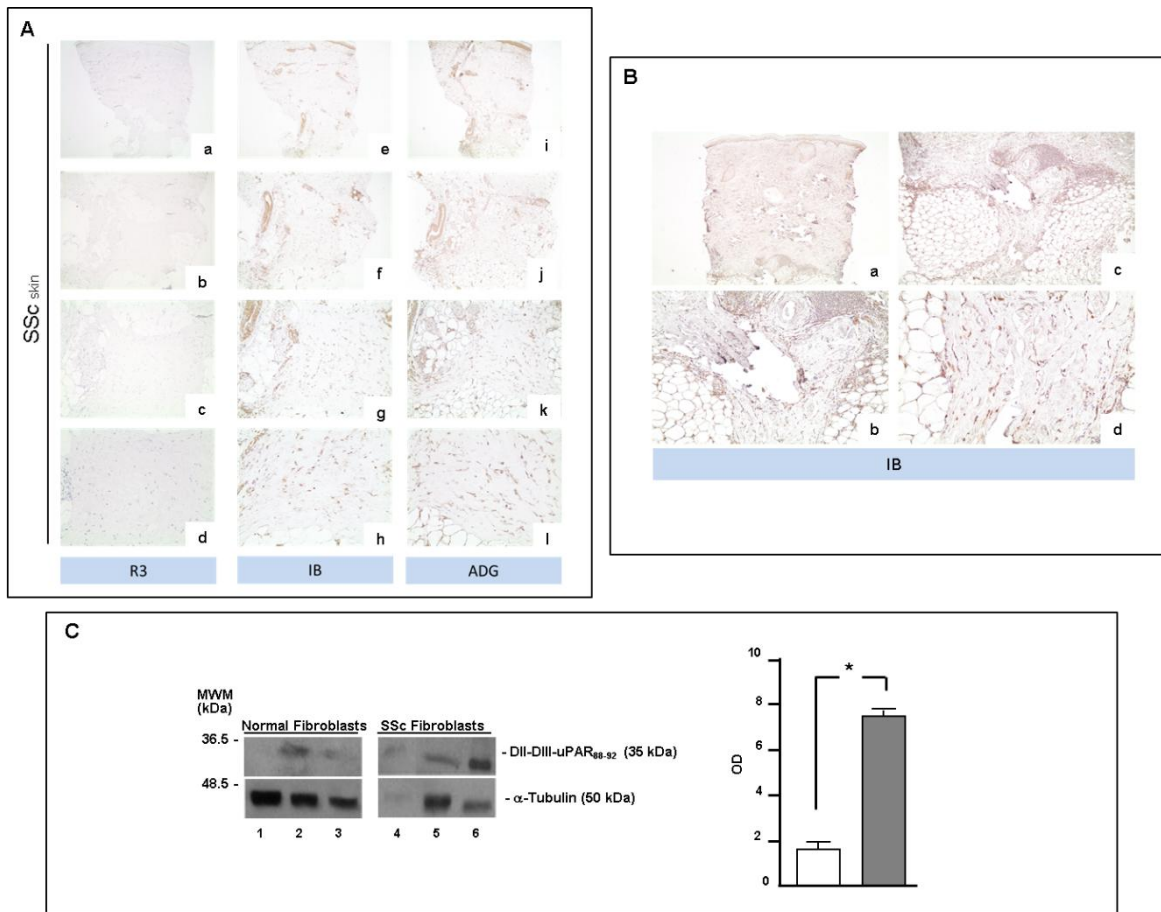


**Figure 6. uPAR expression in normal and SSc skin fibroblasts.**

**A:** (a-d) staining for R3 in localized scleroderma: fibroblasts, lymphocytes and endothelial cells were negative for R3 (a: original magnification, x25; b: original magnification, x50, c: original magnification, x100; d: original magnification, x200); (e-h) staining for IB in localized scleroderma: most fibroblasts, lymphocytes and endothelial cells were positive for IB (f: original magnification, x25; g: original magnification, x50, h: original magnification, x100; i: original magnification, x200); (i-l) staining for ADG in localized scleroderma: weak and focal expression of ADG was observed in fibroblasts, lymphocytes and endothelial cells [k: original magnification, x25; l: original magnification, x50, m: original magnification, x100; n original magnification, x200];

**B:** (a-d) staining for IB on skin biopsy of a localized scleroderma previously evaluated for FPR1, 2 and 3 antibodies expression: fibroblasts, lymphocytes and endothelial cells were positive for IB (a: original magnification, x25; b: original magnification, x50, c: original magnification, x100; d: original magnification, x200).

**C:** Western blot analysis of DII-DIII-uPAR<sub>88-92</sub> expression in normal and SSc skin fibroblasts. Normal (lanes 1–3) and SSc (lanes 4–6) skin fibroblasts were lysed in Triton X-100, and 50  $\mu$ g total protein was analyzed by Western blot with an anti-uPAR<sub>84-95</sub>-specific Ab; three representative cases are shown. Densitometric analysis and normalization to  $\alpha$ -tubulin of the DII-DIII-uPAR<sub>88-92</sub> expression in normal (white column) and SSc fibroblasts (gray column) are also shown.

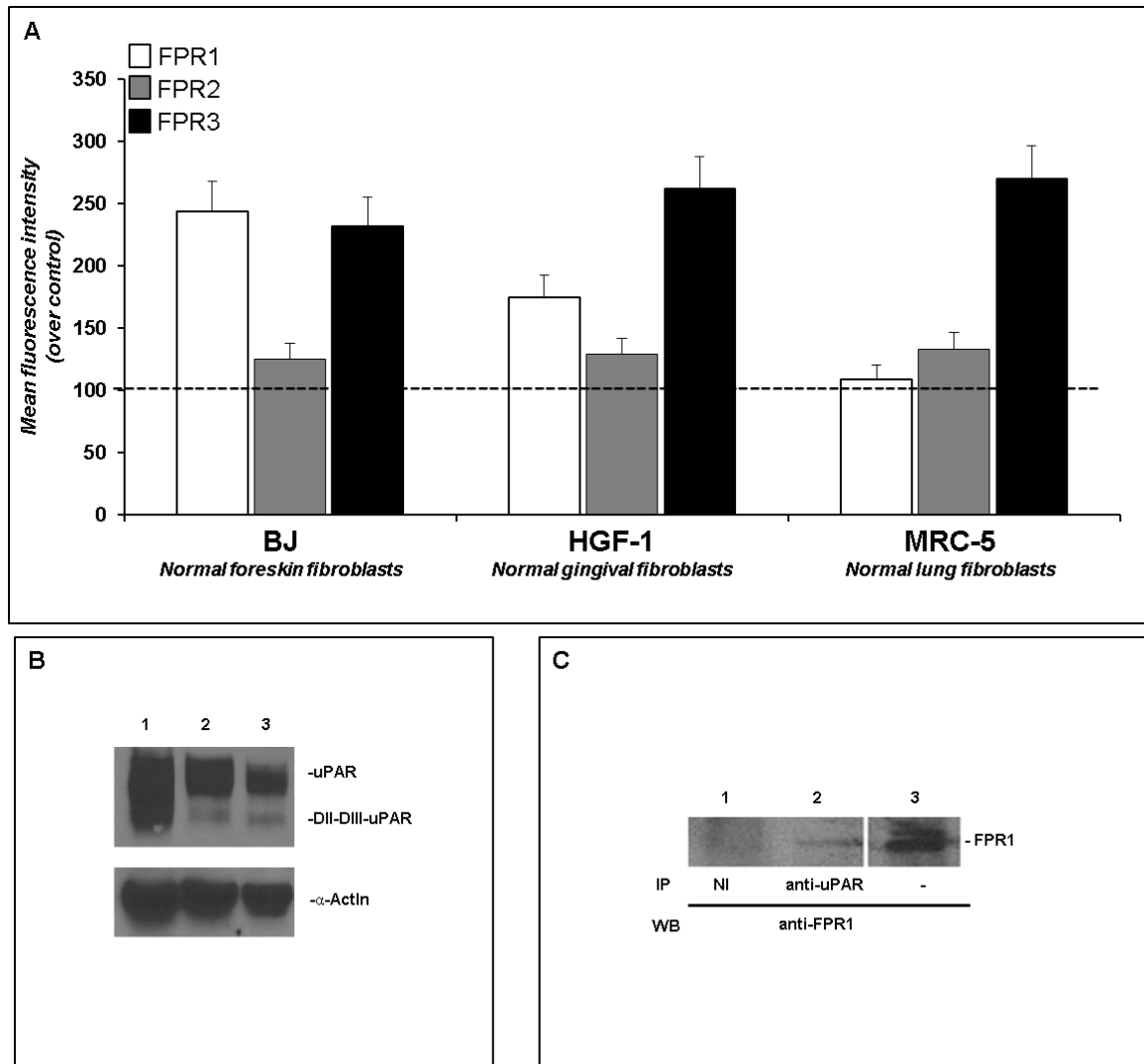


**Figure 7. Expression of FPRs in human normal fibroblasts; uPAR expression and its direct interaction with FPR1 in normal foreskin fibroblast cells.**

**A:** Cytofluorimetric analysis of FPRs expression on human normal fibroblasts. Mean fluorescence intensity of FPR1(white column), FPR2(grey column), and FPR3 (black column) expression in BJ (human normal foreskin fibroblasts), HGF-1 (human normal gingival fibroblasts) and MRC-5 (human normal lung fibroblasts) cells over isotype control.

**B:** Western blot analysis of uPAR expression in H460 cell line as a positive control (lane 1), BJ cell line at 1<sup>st</sup> passage (lane 2) and 5<sup>th</sup> passage (lane 3) in culture. H460 cell line and BJ cell line were lysed in Triton X-100, and 50  $\mu$ g total protein was analyzed by Western blot with the R4 anti-uPAR mAb. and then with  $\alpha$ -actin Ab for loading control.

**C:** uPAR co-immunoprecipitation with FPR1. BJ cell lysates were immunoprecipitated with the R4 anti-uPAR mAb (lane 2) or with nonimmune serum (lane 1). The immunoprecipitated samples were electrophoresed on 10% SDS-PAGE and analyzed by Western blot analysis with an anti-FPR1 Ab. Nonimmunoprecipitated cell lysates were subjected to Western blot analysis with the anti-FPR1 Ab (lane 3) as a loading control.

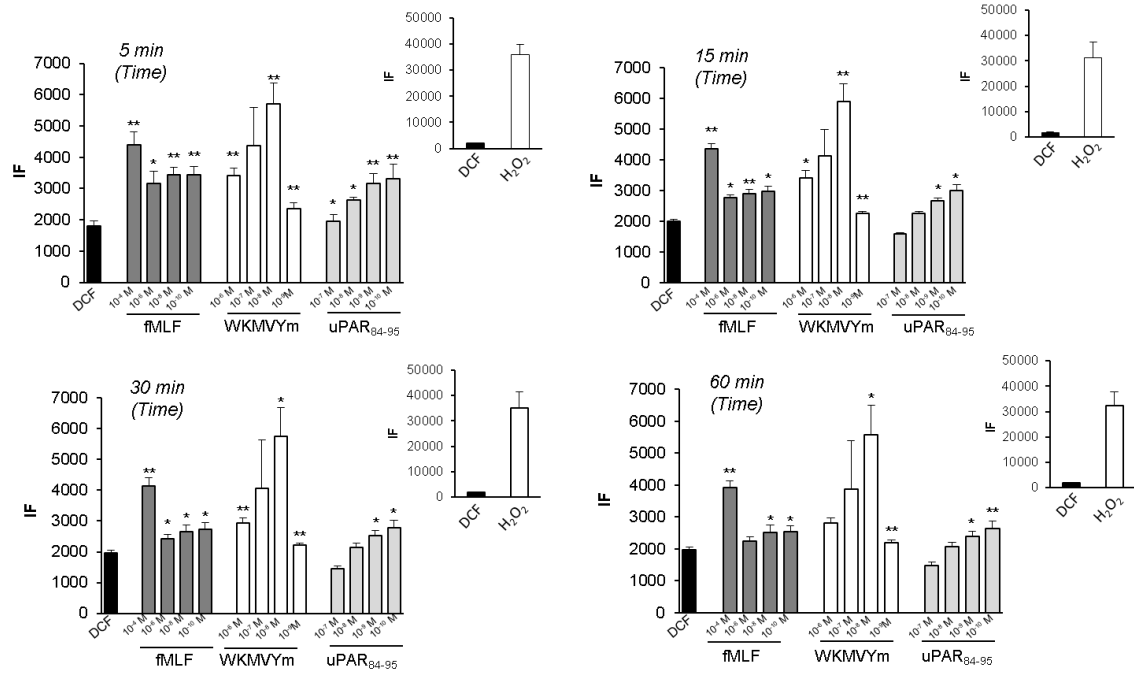


**Figure 8. Effects of fMLF ,WKYMVm peptide and uPAR<sub>84-95</sub> on ROS production in the BJ cell line.** Cells were plated in a 96-well plate and treated with DCHF-DA (5  $\mu$ M) for 30 minutes at 37°C in the dark. At the end of incubation, cells were washed with PBS and treated with medium alone ((black columns), or medium containing fMLF 10<sup>-4</sup> M (grey columns), WKYMVm 10<sup>-8</sup> M peptide (white columns), uPAR<sub>84-95</sub> 10<sup>-8</sup> M (light grey columns). ROS release was measured at a wavelength of 535 nm by a microplate reader (Tecan Trading AG, Switzerland) at 5, 15, 30 and 60 minutes. Results are expressed as mean fluorescence intensity (IF) of DCHF-DA-loaded cells. DCHF-DA-loaded H<sub>2</sub>O<sub>2</sub> unstimulated cells and DCHF-DA-loaded H<sub>2</sub>O<sub>2</sub> stimulated cells were examined in parallel, as controls, and are shown in insets. Values are the mean  $\pm$  SEM of three experiments performed in triplicate. \*p < 0.05; \*\*p < 0.001.

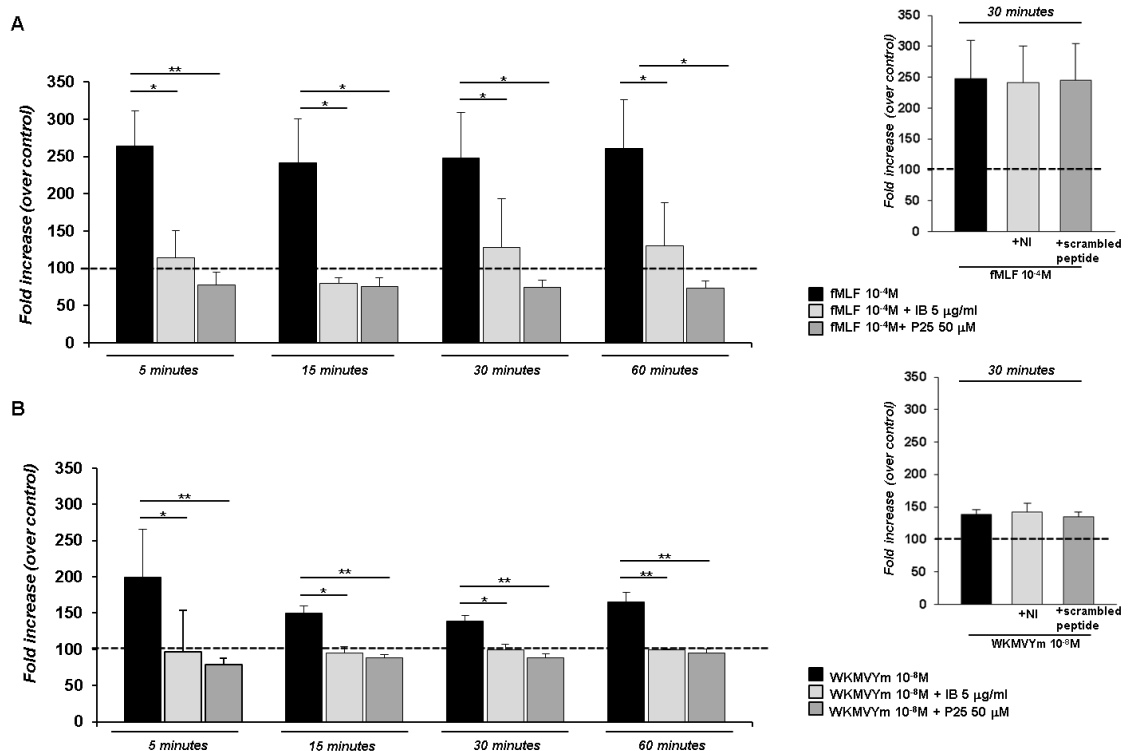


**Figure 9. Effects of the inhibition of the crosstalk between FPRs-uPAR-Integrins on ROS induction in the BJ cell line.**

**A:** Cells were plated in a 96-well plate and treated with DCHF-DA (5 μM) for 30 minutes at 37°C in the dark. At the end of incubation, cells were washed with PBS and treated with medium alone or with fMLF 10<sup>-4</sup> M, in the absence (black columns) or in the presence of 5 μg/ml IB (light grey columns) and of 50 μM P25 (dark grey columns). fMLF 10<sup>-4</sup> M stimulated cells in the absence or in the presence of non immune immunoglobulins and a scrambled peptide, as a negative controls, are shown in the inset.

**B:** Cells were plated in a 96-well plate and treated with DCHF-DA (5 μM) for 30 minutes at 37°C in the dark. At the end of incubation, cells were washed with PBS and treated with medium alone or with WKYMVm 10<sup>-8</sup> M, in the absence (black columns) or in the presence of 5 μg/ml IB (light grey columns) and of 50 μM P25 (dark grey columns). WKYMVm 10<sup>-8</sup> M stimulated cells in the absence or in the presence of non immune immunoglobulins and scrambled peptide, used as a negative controls, are shown in the inset.

ROS release was measured at a wavelength of 535 nm by microplate reader (Tecan Trading AG, Switzerland) at 5, 15, 30, and 60 minutes. Results are expressed as a percentage of mean fluorescence intensity of stimulated DCHF-DA-loaded cells in respect to unstimulated DCHF-DA-loaded cells (considered as 100%). Values are the mean ± SEM of three experiments performed in triplicate. \*p <0.05; \*\*p <0.001.

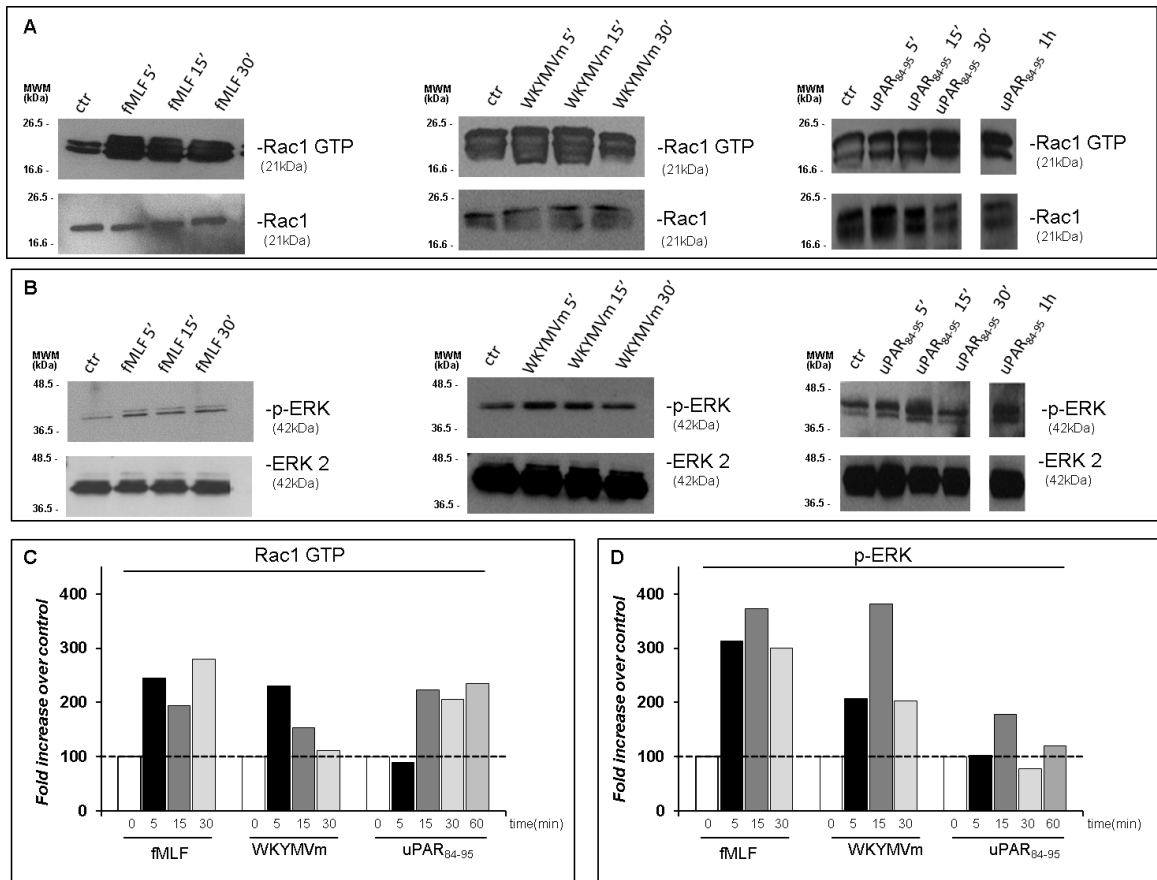


**Figure 10. FPRs-mediated Rac1 and ERK activation in the BJ cell line.**

**A:** Effects of fMLF, WKYMVm peptide and uPAR<sub>84-95</sub> peptide on Rac1 activation. BJ cells, after incubation with fMLF ( $10^{-4}$  M) and with WKYMVm ( $10^{-8}$  M) for 5, 15, and 30 minutes, or with uPAR<sub>84-95</sub> peptide ( $10^{-8}$  M) at 5, 15, 30, and 60 minutes, at 37°C in a humidified (5% CO<sub>2</sub>) incubator, were lysed and subjected to Rac1 activity assay using Pak-PBD-glutathione sepharose beads. Immunoprecipitates and the corresponding total lysates, as loading controls, were subjected to Western blot analysis with an anti Rac1 specific antibody.

**B:** Effects of fMLF, WKYMVm peptide and uPAR<sub>84-95</sub> on Rac1 and ERK activation. BJ cells, after incubation with fMLF ( $10^{-4}$  M) and with WKYMVm ( $10^{-8}$  M) for 5, 15, and 30 minutes, or with uPAR<sub>84-95</sub> ( $10^{-8}$  M) at 5, 15, 30, and 60 minutes, at 37°C in a humidified (5% CO<sub>2</sub>) incubator, were lysed and subjected to Western blot analysis with an anti phospho-ERK 1/2 (p-ERK) specific antibody and with an anti ERK-2 antibody, as a loading control.

**C:** Densitometric analysis and normalization to total Rac1 of Rac1-GTP in BJ cells after treatment with medium alone, fMLF, WKYMVm peptide and uPAR<sub>84-95</sub> peptide.

**D:** Densitometric analysis and normalization to ERK 2 of p-ERK 1/2 in BJ cells after treatment with medium alone, fMLF, WKYMVm peptide and uPAR<sub>84-95</sub>.

5 minutes (Time)

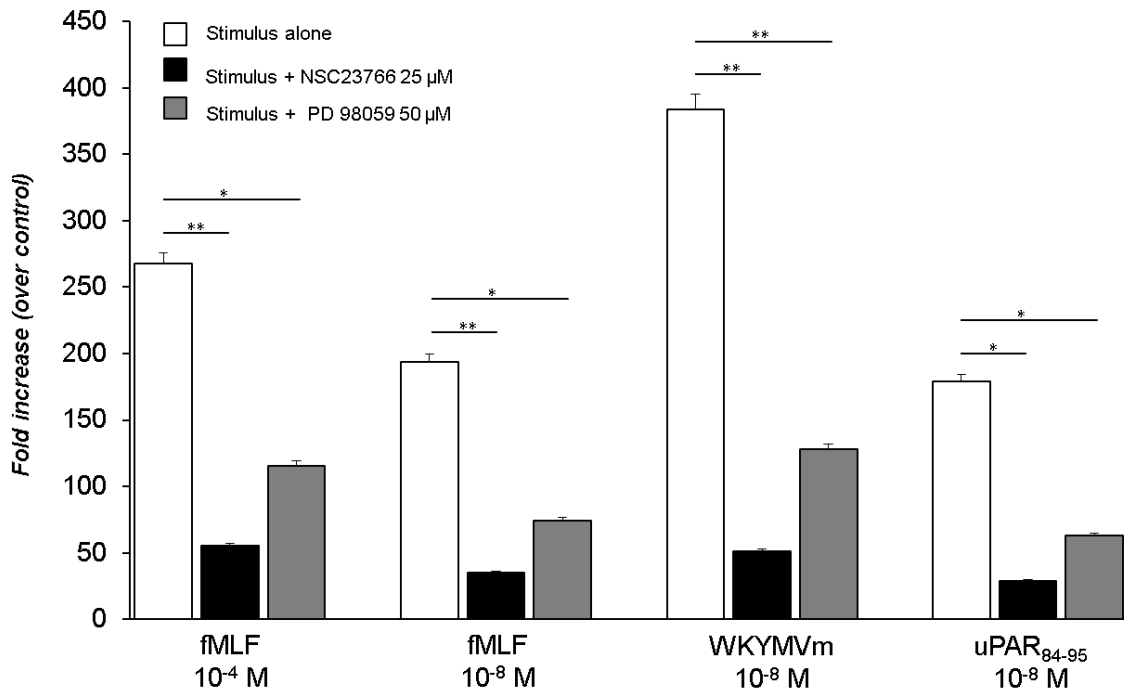


**Figure 11. Effects of Rac1 and ERK inhibition on FPRs-mediated ROS induction in the BJ cell line.** Cells were plated in a 96-well plate and treated with DCHF-DA (5 μM) for 30 minutes at 37°C in the dark. At the end of incubation, cells were washed with PBS and treated with fMLF (10<sup>-4</sup> M), WKYMVm peptide (10<sup>-8</sup> M), or with uPAR<sub>84-95</sub> peptide (10<sup>-8</sup> M), in the absence (white column) or presence of 25 μM NSC23766 (black column) and 50 μM PD98059 (grey column). ROS release was measured at a wavelength of 535 nm by microplate reader (Tecan Trading AG, Switzerland) at 5, 15, 30 and 60 minutes. The 5 minutes time point is shown in the figure; similar results were obtained at increased time points. Results are expressed as a percentage of mean fluorescence intensity of stimulated DCHF-DA-loaded cells in respect to unstimulated DCHF-DA-loaded cells (considered as 100%). Values are the mean ± SEM of three experiments performed in triplicate. \*p < 0.05; \*\*p < 0.001.

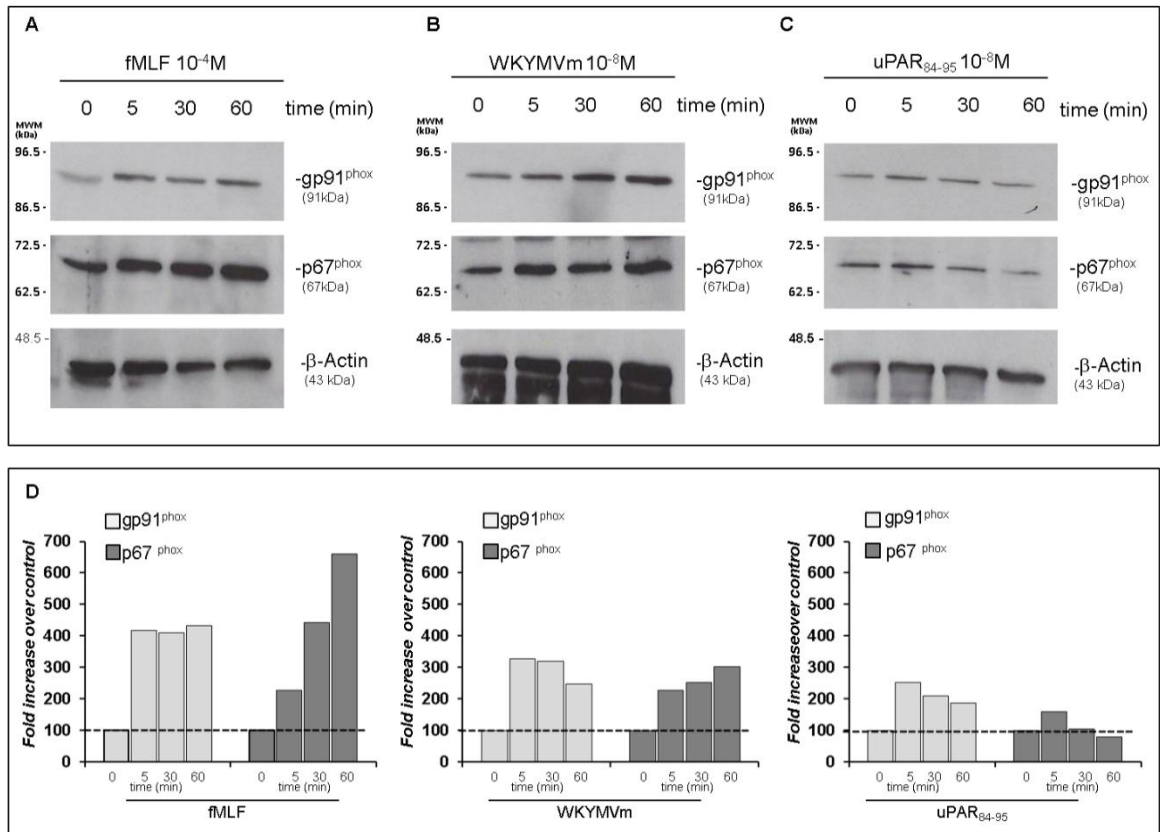


**Figure 12. FPRs modulation of gp91<sup>phox</sup> and p67<sup>phox</sup> expression in the BJ cell line.**

**A:** Western blot analysis with anti-gp91<sup>phox</sup>, -p67<sup>phox</sup> and -β-actin antibodies of BJ cell lysates after incubation with fMLF ( $10^{-4}$  M) for 0, 5, 30, and 60 minutes.

**B:** Western blot analysis with anti-gp91<sup>phox</sup>, -p67<sup>phox</sup> and -β-actin antibodies of BJ cell lysates after incubation with the WKYMVm peptide ( $10^{-8}$  M) for 0, 5, 30, and 60 minutes.

**C:** Western blot analysis with anti-gp91<sup>phox</sup>, -p67<sup>phox</sup> and -β-actin antibodies of BJ cell lysates after incubation with the uPAR<sub>84-95</sub> ( $10^{-8}$  M) peptide for 0, 5, 30, and 60 minutes.

**D:** Normalization to β-actin using densitometric analysis of the gp91<sup>phox</sup> (light grey columns) and p67<sup>phox</sup> (dark grey column) protein levels.

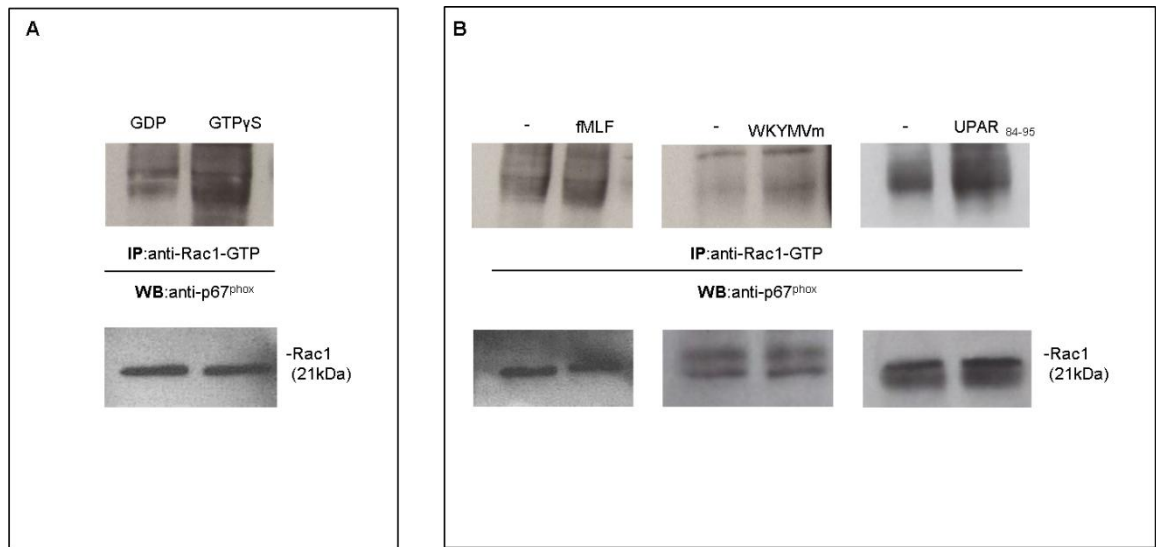


**Figure 13. FPRs-mediated Rac1 GTP-p67<sup>phox</sup> interaction in the BJ cell line.**

**A:** BJ cell lysates were treated with GDP and GTP $\gamma$ S (Upstate) to generate Rac1-GDP and Rac1-GTP, respectively. Active Rac1 (Rac1-GTP) was precipitated from cell lysates using the p21-binding domain (PBD) of its target, PAK1, bound to agarose beads. Eluted samples were subjected to Western blot analysis with a polyclonal anti-p67<sup>phox</sup> antibody.

**B:** BJ cells, after incubation with medium alone (-), fMLF ( $10^{-4}$  M) and WKYMVm peptide ( $10^{-8}$  M) for 5 minutes, or uPAR<sub>84-95</sub> ( $10^{-8}$  M) for 30 minutes at 37°C in a humidified (5% CO<sub>2</sub>) incubator, were lysed and subjected to Rac1 activity assay. Active Rac1 (Rac1-GTP) was precipitated from cell lysates using the p21-binding domain (PBD) of its target, PAK1, bound to agarose beads. Eluted samples were subjected to Western blot analysis with a polyclonal anti-p67<sup>phox</sup> antibody.

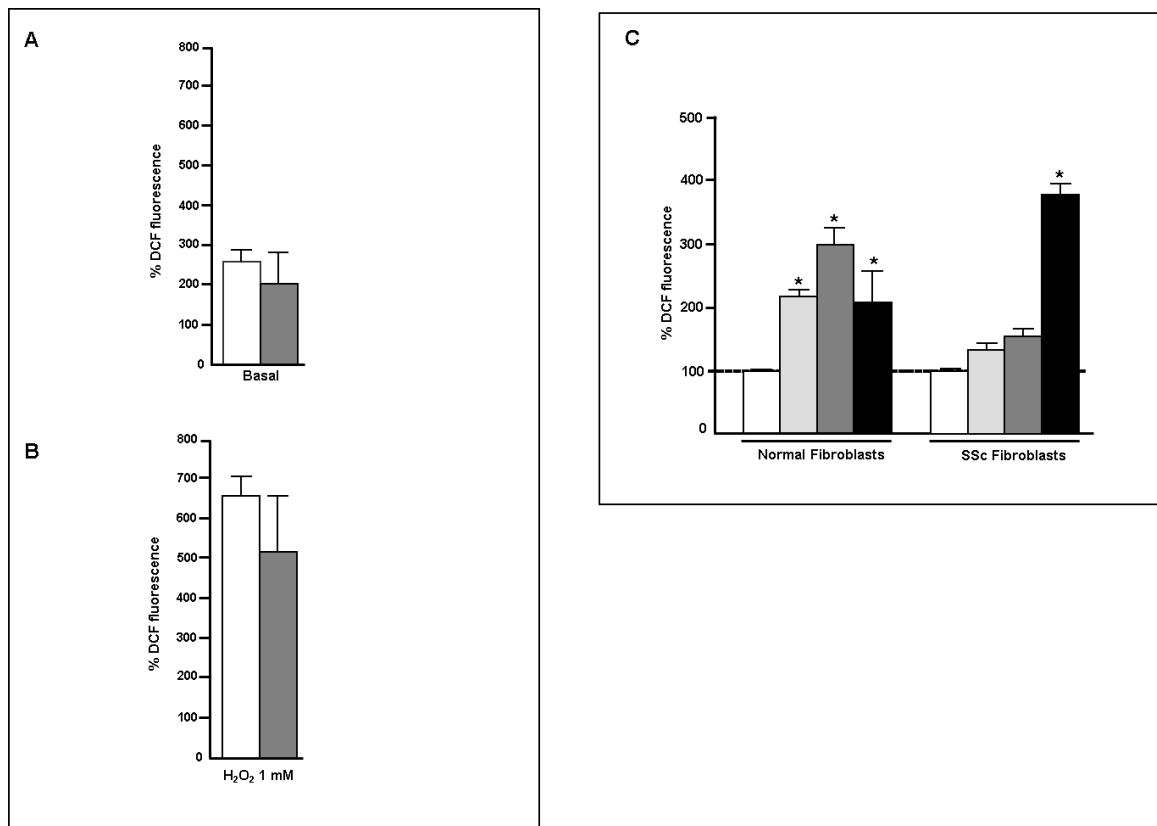


**Figure 14. FPRs-mediated ROS production in human normal and SSc skin fibroblasts.**

**A:** Intracellular oxidation in normal and SSc fibroblasts in basal conditions. Normal ( $n = 10$ , white column) and SSc ( $n = 10$ , gray column) skin fibroblasts were plated in a 6-well plate. Cells were untreated or treated with  $H_2O_2$  (1 mM) for 30 min at  $37^\circ C$  in the dark. At the end of incubation, cells were washed with PBS and loaded with DCHF-DA (5  $\mu M$ ) for 30 min; then, ROS release was measured by flow cytometry at a wavelength of 520 nm (FL1). Results are expressed as percentage of increase of mean fluorescence intensity DCHF-DA-loaded cells, as compared with DCHF-DA-unloaded cells.

**B:** Intracellular oxidation in normal and SSc fibroblasts in response to  $H_2O_2$ . Normal ( $n = 10$ , white column) and SSc ( $n = 10$ , gray column) skin fibroblasts were plated in a 6-well plate. Cells were untreated or treated with  $H_2O_2$  (1 mM) for 30 min at  $37^\circ C$  in the dark. At the end of incubation, cells were washed with PBS and loaded with DCHF-DA (5  $\mu M$ ) for 30 min; then, ROS release was measured by flow cytometry at a wavelength of 520 nm (FL1). Results are expressed as percentage of increase of mean fluorescence intensity of  $H_2O_2$ -stimulated over  $H_2O_2$ -unstimulated cells.

**C:** Effects of ATF-uPA, uPAR<sub>84-95</sub>, and WKYMVm on ROS production in normal and SSc skin fibroblasts. Normal and SSc fibroblasts were treated with medium alone (white column), ATF-uPA ( $10^{-9}$  M) (light gray column), uPAR<sub>84-95</sub> ( $10^{-9}$  M) (dark gray column), and WKYMVm peptide ( $10^{-8}$  M) (black column) for 30 min at  $37^\circ C$  in a humidified 5% CO<sub>2</sub> incubator. Cells were then washed twice, and 5  $\mu M$  DCHF-DA was added for 30 min in the dark at  $37^\circ C$ . At the end of the incubation, cells were washed, trypsinized, and resuspended in PBS for flow cytometric analysis. A total of  $10^4$  events were acquired for each sample in all cytofluorimetric analysis, and intracellular ROS formation was detected as a result of the oxidation of DCHF. DCHF-DA-loaded  $H_2O_2$ -unstimulated cells were considered the 100% of the dichlorofluorescein (DCF) fluorescence. \* $p < 0.05$ .

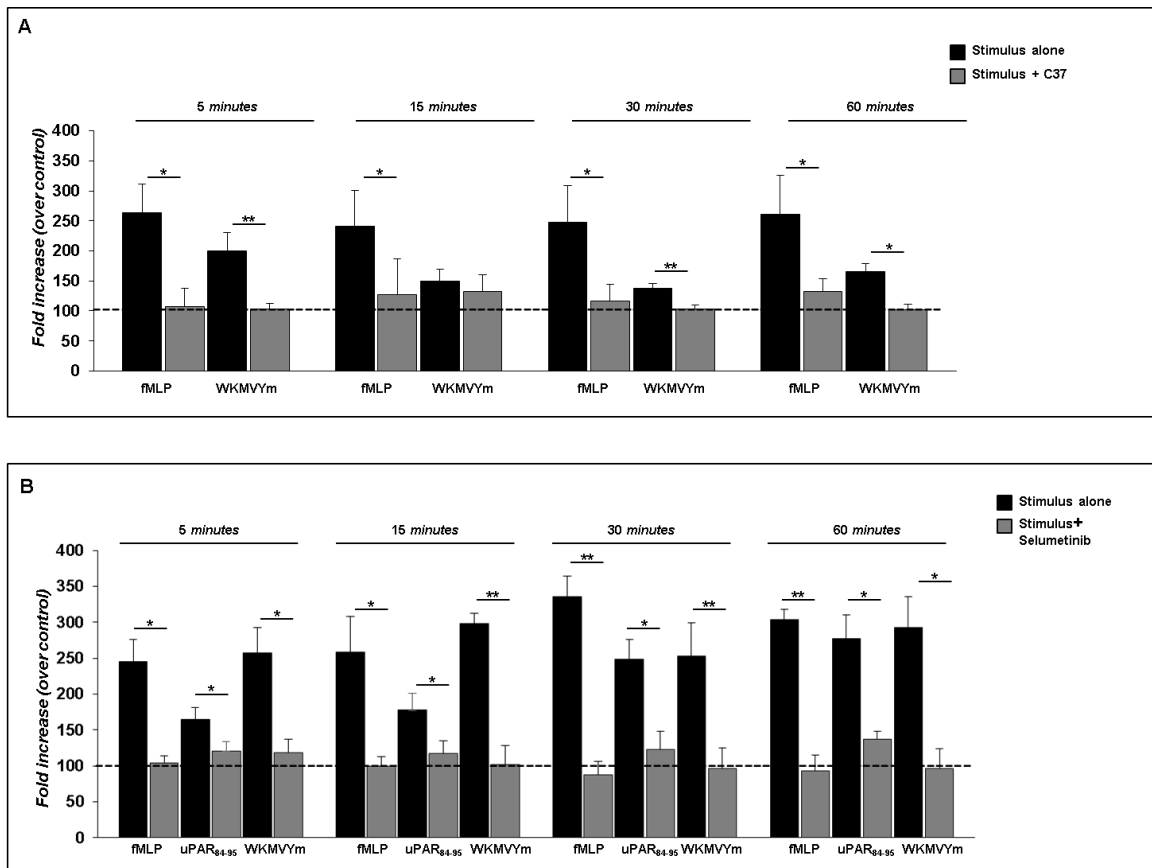


**Figure 15. Effects of C37 and Selumetinib on FPRs-mediated ROS production in the BJ cell line.**

**A:** Cells were plated in a 96-well plate and treated with DCHF-DA (5  $\mu$ M) for 30 minutes at 37°C in the dark. At the end of incubation, cells were washed with PBS and treated with fMLF ( $10^{-4}$  M) and WKVMVYm ( $10^{-8}$  M), in the absence (black column) or presence (grey column) of C37 (10  $\mu$ M). ROS release was measured at a wavelength of 535 nm by microplate reader (Tecan Trading AG, Switzerland) at 5, 15, 30, and 60 minutes. Results are expressed as percentage of increase of mean fluorescence intensity of stimulated DCHF-DA-loaded cells in respect to unstimulated DCHF-DA-loaded cells (considered as 100%).

**B:** Cells were plated in a 96-well plate and treated with DCHF-DA (5 mM) for 30 minutes at 37°C in the dark. At the end of incubation, cells were washed with PBS and treated with fMLF ( $10^{-4}$  M), WKVMVYm ( $10^{-8}$  M), and uPAR<sub>84-95</sub> ( $10^{-8}$  M) in the absence (black column) or presence (grey column) of Selumetinib (2.5  $\mu$ M). ROS release was measured at a wavelength of 535 nm by microplate reader (Tecan Trading AG, Switzerland) at 5, 15, 30, and 60 minutes. Results are expressed as percentage of increase of mean fluorescence intensity of stimulated DCHF-DA-loaded cells in respect to unstimulated DCHF-DA-loaded cells (considered as 100%).

Results are expressed as a percentage of mean fluorescence intensity of stimulated DCHF-DA-loaded cells in respect to unstimulated DCHF-DA-loaded cells (considered as 100%). Values are the mean  $\pm$  SEM of three experiments performed in triplicate. \*p <0.05; \*\*p <0.001.

## 8. REFERENCES

1. Gabrielli A, Avvedimento EV, Krieg T. 2009. Scleroderma. *N Engl J Med.* 360:1989-2003.
2. Jimenez SA and Derk CT. 2004. Following the Molecular Pathways toward an Understanding of the Pathogenesis of Systemic Sclerosis. *Ann Intern Med.* 140:37-50.
3. LeRoy EC, Black C, Fleischmajer R, Jablonska S, Krieg T, Medsger Jr TA, et al. 1988. Scleroderma (systemic sclerosis): classification, subsets and pathogenesis. *J Rheumatol.* 15:202–5.
4. Chiffrot H, Fautrel B, Sordet C, Chatelus E, and Sibilia J. 2008. Incidence and prevalence of systemic sclerosis: a systematic literature review. *Seminars in Arthritis and Rheumatism.* 37:223-235.
5. Manetti M, Guiducci S, and Matucci-Cerinic M. 2011. The origin of the myofibroblast in fibroproliferative vasculopathy: does the endothelial cell steer the pathophysiology of systemic sclerosis? *Arthritis Rheum.* 63:2164–2167.
6. Abraham DJ, Eckes B, Rajkumar V, and Krieg T. 2007. New developments in fibroblast and myofibroblast biology: implications for fibrosis and scleroderma. *Curr Rheumatol Rep.* 9:136–143.
7. Manetti M, Romano E, Rosa I, Guiducci S, Bellando-Randone S, De Paulis A, et al. 2017. Endothelial-to-mesenchymal transition contributes to endothelial dysfunction and dermal fibrosis in systemic sclerosis. *Ann Rheum Dis.* 2016-210229.
8. Amico D, Spadoni T, Rovinelli M, Serafini M, D'Amico G, Campelli N, et al. 2015. Intracellular free radical production by peripheral blood T lymphocytes from patients with systemic sclerosis: role of NADPH oxidase and ERK1/2. *Arthritis Res Ther.* 17:68.
9. Richter K, Kietzmann T. 2016 Reactive oxygen species and fibrosis: further evidence of a significant liaison. *Cell Tissue Res.* 365:591-605.
10. Sambo P, Baroni SS, Luchetti M, Paroncini P, Dusi S, Orlandini G, et al. 2001. Oxidative stress in scleroderma: maintenance of scleroderma fibroblast phenotype by the constitutive up-regulation of reactive oxygen species generation through the NADPH oxidase complex pathway. *Arthr Rheum.* 44:2653–2664.
11. Dooley A, Shi-Wen X, Aden N, Tranah T, Desai N, Denton CP, et al. 2010. Modulation of collagen type I, fibronectin and dermal fibroblast function and activity, in systemic sclerosis by the antioxidant epigallocatechin-3-gallate. *Rheumatology* 49:2024–2036.
12. Bedard K and Krause KH. 2007. The NOX family of ROS-generating NADPH oxidases: physiology and pathophysiology. *Physiol Rev.* 87:245–313.
13. Babior BM. 2004. NADPH oxidase. *Curr Opin Immunol.* 16:42-47.
14. Droge W. 2002. Free radicals in the physiological control of cell function. *Physiol Rev.* 82:47–95.

15. Spadoni T, Svegliati Baroni S, Amico D, Albani L, Moroncini G, Avvedimento EV, et al. 2015. A reactive oxygen species-mediated loop maintains increased expression of NADPH oxidases 2 and 4 in skin fibroblasts from patients with systemic sclerosis. *Arthritis Rheumatol.* 67:1611-22.
16. Luchetti MM, Moroncini G, Jose Escamez M, Svegliati Baroni S, Spadoni T, Grieco A, et al. 2016. Induction of Scleroderma Fibrosis in Skin-Humanized Mice by Administration of Anti-Platelet-Derived Growth Factor Receptor Agonistic Autoantibodies. *Arthritis Rheumatol.* 68:2263-73.
17. Showell HJ, Freer RJ, Zigmond SH, Schiffmann E, Aswanikumar S, Corcoran B, et al. 1976. The structure-activity relations of synthetic peptides as chemotactic factors and inducers of lysosomal secretion for neutrophils. *J Exp Med.* 143:1154–1169.
18. Le Y, Murphy PM, and Wang JM. 2002. Formyl-peptide receptors revisited. *Trends Immunol.* 23:541–548.
19. Ye RD, Boulay F, Wang JM, Dahlgren C, Gerard C, Parmentier M, et al. 2009. International Union of Basic and Clinical Pharmacology. LXXIII. Nomenclature for the formyl peptide receptor (FPR) family. *Pharmacol Rev.* 61:119–161.
20. de Paulis A, Prevete N, Fiorentino I, Walls AF, Curto M, Petraroli A, et al. 2004. Basophils infiltrate human gastric mucosa at sites of *Helicobacter pylori* infection, and exhibit chemotaxis in response to *H. pylori*-derived peptide Hp(2-20). *J Immunol.* 172: 7734–7743.
21. Gao JL, Guillabert A, Hu J, Le Y, Urizar E, Seligman E, et al. 2007. F2L, a peptide derived from heme-binding protein, chemoattracts mouse neutrophils by specifically activating Fpr2, the low-affinity N-formylpeptide receptor. *J Immunol.* 178:1450– 1456.
22. Lee HY, Lee M, Bae YS. 2017. Formyl Peptide Receptors in Cellular Differentiation and Inflammatory Diseases. *J Cell Biochem.* doi: 10.1002/jcb.25877.
23. Oakley RH, Laporte SA, Holt JA, Barak LS, and Caron MG. 1999. Association of beta-arrestin with G protein-coupled receptors during clathrin-mediated endocytosis dictates the profile of receptor resensitization. *J Biol Chem.* 274:32248–32257.
24. Bea YS, Song JY, He R, Ye RD, Kwak JY, et al. 2003. Differential activation of formyl peptide receptor signaling by peptide ligands. *Mol Pharmacol.* 64:841-7.
25. Pan ZK, Chen LY, Cochrane CG, and Zuraw BL. 2000. fMet -Leu-Phe stimulates proinflammatory cytokine gene expression in human peripheral blood monocytes: the role of phosphatidyl-inositol 3-kinase. *J Immunol.* 164:404-41.
26. Cavicchioni G, Fraulini A, Turchetti M, Varani K, Falzarano S, Pavan B, et al. 2005. Biological activity off or-Met-Leu-Phe-OMe analogs: relevant substitutions specifically trigger killing mechanisms in human neutrophils. *Eur. J. Pharmacol.* 512:1-8.
27. Prevete N, Liotti F, Marone G, Melillo RM, de Paulis A. 2015. Formyl peptide receptors at the interface of inflammation, angiogenesis and tumor growth. *Pharmacol Res.* 102:184-91.

28. El-Benna J, Dang PMC, Gougerot-Pocidallo MA, Marie JC and Braut-Boucher F. 2009. p47phox, the phagocyte NADPH oxidase/NOX2 organizer: structure, phosphorylation and implication in diseases. *Exp Mol Med.* 41:217-225.
29. Koga H, Terasawa H, Nunoi H, Takeshige K, Inagaki F, Sumimoto H. 1999. Tetratricopeptide repeat (TPR) motifs of p67phox participate in interaction with the small GTPase Rac and activation of the phagocyte NADPH oxidase. *J Biol Chem.* 274:25051–25060.
30. Grizot S, Fieschi F, Dagher MC, Pebay-Peyroula E. 2001. The active N-terminal region of p67phox: structure at 1.8 Å resolution and biochemical characterizations of the A128V mutant implicated in chronic granulomatous disease. *J Biol Chem.* 276:21627–21631.
31. Zhou Y, Bian X, Le Y, Gong W, Hu J, Zhang X, et al. 2005. Formyl peptide receptor FPR and the rapid growth of malignant human gliomas. *J National Cancer Institute.* 11:823-835.
32. Blasi F., Carmeliet P. 2002. uPAR: a versatile signalling orchestrator. *Nat Rev Mol Cell Biol.* 3:932-43.
33. Ragno P. 2006. The urokinase receptor: a ligand or a receptor? Story of a sociable molecule. *Cell Mol Life Sci.* 63:1028-37.
34. Madsen CD, Sidenius N. 2008. The interaction between urokinase receptor and vitronectin in cell adhesion and signalling. *Eur J Cell Biol.* 87:617-29.
35. Crippa MP. 2007. Urokinase-type plasminogen activator. *Int J Biochem Cell Biol* 39:690-694.
36. Jo M, Takimoto S, Montel V, Gonias SL. 2009. The urokinase receptor promotes cancer metastasis independently of urokinase-type plasminogen activator in mice. *Am J Pathol.* 175:190-200.
37. Montuori N, Ragno P. 2009. Multiple activities of a multifaceted receptor: roles of cleaved and soluble uPAR. *Front Biosci.* 14:2494-503.
38. Smith HW, Marshall CJ. 2010. Regulation of cell signalling by uPAR. *Nat Rev Mol Cell Biol.* 11:23-36.
39. Degryse B, Resnati M, Czekay RP, Loskutoff DJ, Blasi F. 2005. Domain 2 of the urokinase receptor contains an integrin-interacting epitope with intrinsic signaling activity: generation of a new integrin inhibitor. *J Biol Chem.* 280:24792-803.
40. Chaurasia P, Aguirre-Ghiso JA, Liang OD, Gardsvoll H, Ploug M, Ossowski L. 2006. A region in urokinase plasminogen receptor domain III controlling a functional association with alpha5beta1 integrin and tumor growth. *J Biol Chem.* 281:14852-63.
41. Montuori N, Carriero MV, Salzano S, Rossi G, Ragno P. 2002. The cleavage of the urokinase receptor regulates its multiple functions. *J Biol Chem.* 277:46932-46939.
42. Resnati M, Guttinger M, Valcamonica S, Sidenius N, Blasi F, Fazioli F. 1996. Proteolytic cleavage of the urokinase receptor substitutes for the agonist-induced chemotactic effect. *EMBO J.* 15,1572-82.

43. de Paulis A, Montuori N, Prevete N, Fiorentino I, Rossi FW, Visconte V, et al. 2004. Urokinase induces basophil chemotaxis through a urokinase receptor epitope that is an endogenous ligand for formyl peptide receptor-like 1 and -like 2. *J Immunol.* 173:5739-48.
44. Resnati M, Pallavicini I, Wang JM, Oppenheim J, Serhan CN, Romano M, et al. 2002. The fibrinolytic receptor for urokinase activates the G protein-coupled chemotactic receptor FPRL1/LXA4R *Proc Natl Acad Sci U S A.* 99:1359-64.
45. van den Hoogen F, Khanna D, Fransen J, Johnson SR, Baron M, Tyndall A, et al. 2013. 2013 classification criteria for systemic sclerosis: an American College of Rheumatology/European League against Rheumatism collaborative initiative. *Arthritis Rheum.* 65:2737–2747.
46. Manetti M, Guiducci S, Romano E, Rosa I, Ceccarelli C, Mello T, et al. 2013. Differential expression of junctional adhesion molecules in different stages of systemic sclerosis. *Arthritis Rheum.* 65:247–2.
47. Postiglione L, Montuori N, Riccio A, Di Spigna G, Salzano S, Rossi G, et al. 2010. The plasminogen activator system in fibroblasts from systemic sclerosis. *Int. J Immunopathol Pharmacol.* 23:891–900.
48. Svensson L, Redvall E, Björn C, Karlsson J, Bergin A M, Rabiet MJ, et al. 2007. House dust mite allergen activates human eosinophils via formyl peptide receptor and formyl peptide receptor-like 1. *Eur J Immunol.* 37:1966-77.
49. Snedecor GW and Cochran WG. 1980. Statistical methods, 7th Ed. Iowa State University Press, Ames, IA.
50. D'Alessio S, Fibbi G, Cinelli M, Guiducci S, Del Rosso A, Margheri F, et al. 2004. Matrix metalloproteinase 12 dependent cleavage of urokinase receptor in systemic sclerosis microvascular endothelial cells results in impaired angiogenesis. *Arthritis Rheum.* 50:3275–3285.
51. Manetti M, Rosa I, Milia AF, Guiducci S, Carmeliet P, Ibba-Manneschi L, et al. 2014 Inactivation of urokinase-type plasminogen activator receptor (uPAR) gene induces dermal and pulmonary fibrosis and peripheral microvasculopathy in mice: a new model of experimental scleroderma? *Ann Rheum Dis.* 73:1700-9.
52. Ronne E, Behrendt N, Ellis V, Ploug M, Dano K, and Hoyer-Hansen G. 1991. Cell-induced potentiation of the plasminogen activation system is abolished by a monoclonal antibody that recognizes the NH2-terminal domain of the urokinase receptor. *FEBS Lett.* 288:233-236.
53. Montuori N, Bifulco K, Carriero MV, La Penna C, Visconte V, Alfano D, et al. 2011. The crosstalk between the urokinase receptor and fMLP receptors regulates the activity of the CXCR4 chemokine receptor. *Cell Mol Life Sci.* 68: 2453–2467.
54. Bodnar AG, et al. 1998. Extension of life-span by introduction of telomerase into normal human cells. *Science.* 279:349-352.
55. Gorrasi A, Li Santi A, Amodio G, Alfano D, Remondelli P, Montuori N, et al. 2014. The urokinase receptor takes control of cell migration by recruiting integrins and FPR1 on the cell surface. *PLoS One* 9:e86352.

56. Bifulco K, Votta G, Ingangi V, Di Carluccio G, Rea D, Losito S, et al. 2014. Urokinase receptor promotes ovarian cancer cell dissemination through its 84-95 sequence. *Oncotarget* 5:4154–4169.
57. Rossi FW, Napolitano F, Pesapane A, Mascolo M, Staibano S, Matucci-Cerinic M, et al. 2015. Upregulation of the N-Formyl Peptide Receptors in Scleroderma Fibroblasts Fosters the Switch to Myofibroblasts. *J Immunol.* 194:5161-73.
58. Valko M, Leibfritz D, Moncol J, Cronin MT, Mazur M, Telser J. 2007. Free radicals and antioxidants in normal physiological functions and human disease. *Int J Biochem Cell Biol.* 39:44-84.
59. Miller AA, Drummond GR, and Sobey CG. 2006 Reactive Oxygen Species in the Cerebral Circulation: Are They All Bad? *Antioxidants & Redox Signaling.* 8: 1113-1120.
60. Leoni G, Alam A, Neumann PA, Lambeth JD, Cheng G, McCoy J, et al. 2013. Annexin A1, formyl peptide receptor, and NOX1 orchestrate epithelial repair. *J Clin Invest.* 123:443-54.
61. Wei Y, Lukashev M, Simon DI, Bodary SC, Rosenberg S, et al. 1996. Regulation of integrin function by the urokinase receptor. *Science.* 273: 1551–5.
62. Lapouge K, Smith SJ, Walker PA, Gamblin SJ, Smerdon SJ, Rittinger K. 2000. Structure of the TPR domain of p67phox in complex with Rac GTP. *Mol Cell.* 6:899-907.
63. Svegliati S, Canello R, Sambo P, et al. 2005. Platelet-derived growth factor and reactive oxygen species (ROS) regulate Ras protein levels in primary human fibroblasts via ERK1/2: amplification of ROS and Ras in systemic sclerosis fibroblasts. *J Biol Chem.* 280:36474-82.
64. Spadoni T, Svegliati Baroni S, Amico D, Albani L, Moroncini G, Avvedimento EV, Gabrielli A. 2015. A reactive oxygen species-mediated loop maintains increased expression of NADPH oxidases 2 and 4 in skin fibroblasts from patients with systemic sclerosis. *Arthritis Rheumatol.* 67:1611-22.
65. Rea VE, Lavecchia A, Di Giovanni C, Rossi FW, Gorrasi A, Pesapane A, de Paulis A, Ragno P, Montuori N. 2013. Discovery of New Small Molecules Targeting the Vitronectin-Binding Site of the Urokinase Receptor That Block Cancer Cell Invasion. *Mol Cancer Ther.* 12:1402-16.
66. Madala SK, Schmidt S, Davidson C, Ikegami M, Wert S, Hardie WD 2011. MEK-ERK pathway modulation ameliorates pulmonary fibrosis associated with epidermal growth factor receptor activation. *Am J Respir Cell Mol Biol.* 46:380-8.
67. Iwamoto N, Vettori S, Maurer B, Brock M, Pachera E, Jüngel A, et al. 2016. Downregulation of miR-193b in systemic sclerosis regulates the proliferative vasculopathy by urokinase-type plasminogen activator expression. *Ann Rheum Dis.* 75:303-10.